STRESS ANALYSIS OF LAMINATED COMPOSITE BEAM WITH I-SECTION

by

JITESH CHERUKKADU PARAMBIL

Presented to the Faculty of the Graduate School of

The University of Texas at Arlington in Partial Fulfillment

of the Requirements

for the Degree of

MASTER OF SCIENCE IN AEROSPACE ENGINEERING

THE UNIVERSITY OF TEXAS AT ARLINGTON

MAY 2010

To my dear father, mother, sister, and brother for

their support throughout my life

ACKNOWLEDGEMENTS

I would first like to thank my supervising Professor, Dr. Kent L. Lawrence, and Co-supervising Professor, Dr. Wen S. Chan for whom I have the deepest admiration, for their continuous guidance and encouragement throughout the duration of this thesis. Their faith and belief in my abilities helped me accomplish my thesis work.

I would also like to express my gratitude to Dr. Stefan D. Dancila for taking time to serve on my committee. I would like to thank Dr. Dereje Agonafer for allowing me to use EMNSPC lab to carry out my ANSYS simulations. I would like to thank all my family and friends for their support through these years.

April 19, 2010

ABSTRACT

STRESS ANALYSIS OF LAMINATED COMPOSITE BEAMS

WITH I-SECTION

Jitesh Cherukkadu Parambil, M S

The University of Texas at Arlington, 2010

Supervising Professors: Kent L. Lawrence, Wen S. Chan

The advantage of material properties and flexibility of choosing material have made composite materials a primary preference for structural application. Unlike isotropic materials, the parametric study of composite beams for optimized design is complicated due to high number of parameters involved in designing like lay-up sequence, and layer configuration. Moreover, the limitations of FEA techniques in designing have created a need for an analytical closed-form solution for stress analysis of laminated composite beams. The objective of this study focuses on the development of an analytical method for stress analysis of composite I-beam.

This method includes the structural response due to unsymmetrical and/or unbalanced of laminate as well as unsymmetrical I-beam cross-section. These structural characteristics are often ignored in the most published studies. Analytical closed-form expressions for the sectional properties such as centroid, axial and bending stiffnesses of composite I-beam are derived. These sectional properties are then used to calculate the stress and strain of each ply of I-beam

at any given location. Further, a finite element model is created using commercial software ANSYS 11.0 classic. The stress and strain results obtained by analytical method have excellent agreement with the results obtained from the finite element analysis.

TABLE OF CONTENTS

LIST OF ILLUSTRATIONS

LIST OF TABLES

CHAPTER 1

INTRODUCTION

1.1 Composite Material Overview

Composite materials have been used in the industry for many years because they perform better than the comparable homogenous isotropic materials. Advanced composites like fiber reinforced composite are widely used in aerospace industry. The advantages of composite such as high specific strength and stiffness, good corrosion resistance, and lower thermal expansion make them a primary preference in aircraft structures and other applications. The designer's freedom to choose from various basic constituents to achieve properties for a particular application makes them attractive option for design.

With development of composites and the need for advanced materials for aircraft industry; the use of composites in aircraft structures has significantly increased. Composite load carrying structures like aircraft wings, skin, tail planes have solid stiffeners for efficient load bearing abilities. The composite thin-walled beams like I-beams are extensively used as chief structural elements. Moreover, the anisotropic nature of the composite materials makes it difficult to predict the structural behavior under loading. The FEA techniques are being employed to assist the designer in finding an optimized solution. However, FEA techniques are cumbersome, non-economical in terms of time and money when designing parameters are large in numbers. For example, in a case of a parametric study for different options of cross-section, layer configuration and lay-up sequence an analytical solution would be more appropriate than a FEA solution. Therefore, a need to develop an efficient analytical method to analyze composite beams is required for optimized designing of thin-walled beams

1.2 Literature Review

There have been numerous research published in the area of composite beams. In this section, the review on composite study is focused on analytical studies and finite element analysis. In an early study on composite by Barbero et al. [1] focused on ultimate bending strength of composite beams under bending. The study compared the experimental and analytical solution and found that glass fiber reinforced plastic (GFRP) beam attained ultimate bending strength as the result of local buckling of the compression in flange. Drummond and Chan [2] analytically and experimentally investigated bending stiffness of composite I-beam including spandrels at the intersection of flange and web. In their study, they found the calculated bending stiffness for narrow I-beam, $1/d_{11}$ instead of D_{11} has the smaller difference from both experimental and FEM results.

In their study of bending stiffness of laminate I-beams, Craddock, and Yen [3] obtained equivalent bending stiffness of I-beams with symmetrical cross-section. The authors ignored the laminate stiffness due to Poisson's ratio and coupling by only using A_{11} (axial stiffness) for the calculation of bending stiffness.

In another study on composite I-beams, Chandra and Chopra [4] presented a comparative study of experimental and theoretical data to understand the static response on composite I-beams. A Vlasov-type linear theory was developed for open section beams which included the transverse shear deformation. They analyzed the structural response by measuring bending slope and twist for I-beam under tip loading and torsional load. In addition to this, authors evaluated torisional stiffness and extensional stiffness (ES) with and without shear deformation effect. The work also included the effect of slenderness ratio, constrained warping effect, fiber orientation and stacking sequence. The authors concluded that the transverse shear decreases the extensional stiffness and the reduction depends on the stacking of layer in the beam. They also concluded that the transverse shear deflection have insignificant importance on the structural response on symmetrical I-beams in loading.

Barbero et al. [5] in an attempt to predict a design optimization approach for different shapes presented derivation on Mechanics of thin-walled Laminated Beams (MLB) for open and closed sections. The authors presented the example of laminated I-beam and developed the deflection equation for cantilevered beam. The tip deflection equation incorporated the effects of shear deformation by including a shear correction factor term in the equation. However, the bending stiffness term was direct reciprocal of compliance matrix. Therefore, the bending stiffness only represented the smeared material property of the laminate.

In a study to understand static response of I-beams, Song et al. [6] presented an analytical solution for end deflection in I-beams loaded at their free end. Two fundamental configurations were considered for the analyses. First, circumferentially uniform stiffness (CUS) configuration results in bending-twist and extension-shear couplings. Second, circumferentially asymmetric stiffness (CAS) results in extension-twist and bending-shear elastic couplings. These two configurations were analyzed for non-classical effect such as directionality property of materials, transverse shear effect, and warping effect. For CAS beam configuration they found that transverse shear effects are higher in flapping than in the lagging degree of freedom. However for CUS beam configuration, the lagging displacement increases with the increase in ply angle i.e. it increases with the increase of lagging-transverse shear stiffness coupling. In addition, the flapping deflection decreases with increase in ply angle.

Jung and Lee [7] presented a study on the static response and performed a closed form analysis of thin walled composite I-beams. The analysis included the non-classical effects such as elastic coupling, shell wall thickness, transverse shear deformation, torsion warping, and constrained warping. The closed form solution was derived for both symmetric and anti-symmetric layup configuration for a cantilever beam subjected to unit bending or torque load at the tip of the beam. In addition, 2D finite element model was developed to validate the results obtained from the closed form solution. They concluded that transverse shear deformation influences the structural behavior of composite beams in terms of slenderness ratio and layup

geometry of the beams. The results point out that transverse shear effect is higher in anti-symmetry than in symmetric beams.

In analysis of composite beam, the sectional properties of beam cross-section are often obtained by using smear property of laminate. Then the conventional method used for isotropic material is employed. In this approach, the structural response due to unsymmetrical and unbalanced layups as well as unsymmetrical cross-section is ignored. Chan and Chou [8] developed a closed form for axial and bending stiffness that included this effect. Later, Chan and his students focused on thin-walled beams for various cross sections. In one of the study, Chan and Dermirhan [9] developed a closed form solution for calculating the bending stiffness of composite tubular beam. The study compared the solution with smeared property approach to indicate the difference in evaluating methods and approximation involved. Later, Rojas and Chan [10] in a study integrated an analysis of laminates including calculation of structural section properties, failure prediction, and analysis of composite laminated beams. Syed and Chan [11] obtained a closed expression for computing centroid location, axial and, bending stiffnesses as well as shear center of hat-section composite beam. Most recently, Rios [12] presented a unified analysis of stiffener reinforced composite beams. The study presented a general analytical method to study the structural response of composite laminated beams.

Finite element analysis has been useful and considered an accurate to develop 3D model simulating similar boundary and loading condition compared to the real-life problems. Several research papers have been published on finite element modeling of composite I-beam. Shell elements are commonly employed to model composite structures in two dimensions. Jung and Lee [7] studied composite I-beam using 2D shell element, 4-noded plate/shell element of MSC/NASTRAN. The slenderness ratio of the beam was kept within 20 for accurate results. Similarly, Barbero et al. [5] developed a finite element model using 8-node isoparametric laminate shell elements in ANSYS for refined Finite Element Analysis (FEA).

A three dimensional model of composite I-beam was developed by Gan et al [13]. The model was developed by using three dimensional solid elements with composite material properties. Half section of the section was modeled due to the symmetry. Elements with 8-nodes and 20-nodes were used for global and local analyses, respectively..

1.3 Objective and Approach to the thesis

The primary objective of this research is to effectively conduct stress analysis of a composite I-beam. For stress analysis of I-beam, an analytical expression is developed for calculating sectional properties like centroid, equivalent axial and bending stiffnesses of composite I-section beam. The study then focuses on the procedure to calculate stresses and strains of each layer in flange and web laminates.

A 3D finite element model of composite I-beam is developed in ANSYS 11.0 to determine the stresses and strains. The model is also used to validate and compare the results from analytical expression.

This study is intended to provide tools that ensure better designing options for composite laminates.

1.4 General Outline

Chapter 2 describes the general constitutive equation and fundamentals of lamination theory. Laminate specific constitutive equations are developed depending on the boundary and loading condition.

Chapter 3 describes in detail the development of analytical expression for the sectional properties for the composite I-beam. The chapter also focuses on development of analytical expression for the deflection of composite beam at free end under cantilever configuration.

The step wise procedure to develop the finite element model is presented in Chapter 4. The analytical solution developed is validated using the finite element model in Chapter 5. This chapter also discusses the stress and strain obtained in different plies and result comparison

between the analytical and finite element methods. Finally, Chapter 6 summarizes the results and depicts the future study.

CHAPTER 2

CONSTITUTIVE EQUATION FOR LAMINATED COMPOSITE BEAM

The chapter describes the general constitutive equation of laminated plate, so called ‘lamination theory’. The chapter also describes the development of constitutive equation for laminated composite I-beam. The constitutive equation is developed individually for the top, bottom and web laminates depending on the boundary conditions and behavior under the loading conditions.

2.1 Coordinate System for Lamina and Laminates

A laminate is made up of perfectly bonded layers of lamina with different fiber orientation to represent an integrated structural component. In most practical applications of composite material, the laminates are considered as thin and loaded along the plane of laminates. A thin orthotropic unidirectional lamina as depicted in Figure 2.1 has fiber orientation along the 1-direction and the direction transverse to the fiber along the 2-direction. The x-y coordinates represent the global coordinate system for the lamina.

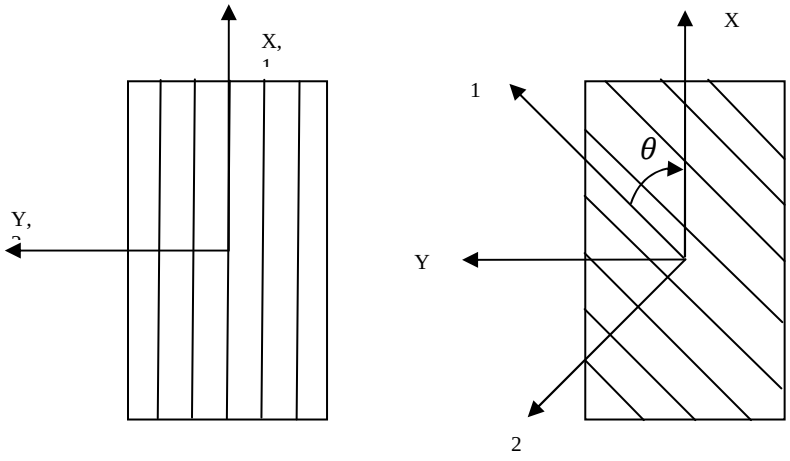

Figure 2.1 Coordinates of Lamina.

2.2 Lamina Constitutive Equation

2.2.1 Stress-Strain Relationship for 0^0 Lamina

Since the lamina is thin, the state of stress can be considered in the plane stress condition. That means,

$$\sigma_3 = 0$$

$$\tau_{23} = 0 \tag{2.1}$$

$$\tau_{13} = 0$$

Hence, the stress-strain relationship for thin lamina in the matrix form along the principal axis can be written as,

$$[\varepsilon]_{1-2} = \begin{bmatrix} \varepsilon_1 \\ \varepsilon_2 \\ \gamma_{12} \end{bmatrix} = \begin{bmatrix} S_{11} & S_{12} & 0 \\ S_{12} & S_{22} & 0 \\ 0 & 0 & S_{66} \end{bmatrix} \begin{bmatrix} \sigma_1 \\ \sigma_2 \\ \tau_{12} \end{bmatrix} \tag{2.2}$$

The elements in compliance matrix $[S]$ are the functions of elastic constant of the composite lamina and can be expressed as,

$$S_{11} = \frac{1}{E_1}$$

$$S_{22} = \frac{1}{E_2}$$

$$S_{12} = -\frac{\nu_{12}}{E_1} = -\frac{\nu_{21}}{E_2}$$

$$S_{66} = \frac{1}{G_{12}} \tag{2.3}$$

Inverting Equation (2.2) we have,

$$[\sigma]_{1-2} = \begin{bmatrix} \sigma_1 \\ \sigma_2 \\ \tau_{12} \end{bmatrix} = \begin{bmatrix} Q_{11} & Q_{12} & 0 \\ Q_{12} & Q_{22} & 0 \\ 0 & 0 & Q_{66} \end{bmatrix} \begin{bmatrix} \varepsilon_1 \\ \varepsilon_2 \\ \gamma_{12} \end{bmatrix} \tag{2.4}$$

The elements in stiffness matrix $[Q]$ can be expressed as,

$$Q_{11} = \frac{E_1}{1 - \nu_{12}\nu_{21}}$$

$$Q_{22} = \frac{E_2}{1 - \nu_{12}\nu_{21}}$$

$$Q_{12} = \frac{\nu_{21}E_1}{1 - \nu_{12}\nu_{21}} = \frac{\nu_{12}E_2}{1 - \nu_{12}\nu_{21}}$$

$$Q_{66} = G_{12}$$

(2.5)

2.2.2 Stress-Strain Transformation Matrices

Generally, the lamina reference axes (x, y) do not coincide with the lamina principle axes (1, 2). Therefore, the relation between the stress and strain components in principal axes making an angle θ with respect to reference axes can be expressed using transformation matrices as,

$$[\sigma]_{1-2} = [T_\sigma][\sigma]_{x-y}$$

and

$$[\varepsilon]_{1-2} = [T_\varepsilon][\varepsilon]_{x-y} \quad (2.6)$$

where $[T_\sigma]$and $[T_\varepsilon]$ are the transformation matrices for stress and strain, respectively. They are

$$[T_\sigma] = \begin{bmatrix} m^2 & n^2 & 2mn \\ n^2 & m^2 & -2mn \\ -mn & mn & m^2 - n^2 \end{bmatrix}$$

and

$$[T_\sigma] = \begin{bmatrix} m^2 & n^2 & mn \\ n^2 & m^2 & -mn \\ -2mn & 2mn & m^2 - n^2 \end{bmatrix}$$

(2.7)

where $m = Cos\theta$ and $n = Sin\theta$

2.2.3 Stress-Strain Relationship for θ^0 Lamina

The stress-strain relationship for thin lamina in the matrix form along the global x-y axis is given as

$$\begin{bmatrix} \sigma_x \\ \sigma_y \\ \tau_{xy} \end{bmatrix} = \begin{bmatrix} \overline{Q_{11}} & \overline{Q_{12}} & \overline{Q_{16}} \\ \overline{Q_{21}} & \overline{Q_{22}} & \overline{Q_{26}} \\ \overline{Q_{61}} & \overline{Q_{62}} & \overline{Q_{66}} \end{bmatrix} \begin{bmatrix} \varepsilon_x \\ \varepsilon_y \\ \gamma_{xy} \end{bmatrix} \tag{2.8}$$

Where the elements in the stiffness matrix, $[\bar{Q}]$ matrix are

$$\overline{Q_{11}} = m^4 Q_{11} + n^4 Q_{22} + 2m^2 n^2 Q_{12} + 4m^2 n^2 Q_{66}$$

$$\overline{Q_{22}} = n^4 Q_{11} + m^4 Q_{22} + 2m^2 n^2 Q_{12} + 4m^2 n^2 Q_{66}$$

$$\overline{Q_{12}} = \overline{Q_{21}} = m^2 n^2 (Q_{11} + Q_{22} - 4Q_{66}) + (m^4 + n^4) Q_{12}$$

$$\overline{Q_{16}} = \overline{Q_{61}} = m^3 n (Q_{11} - Q_{22} - 2Q_{66}) + mn^3 (Q_{12} - Q_{22} + 2Q_{66})$$

$$\overline{Q_{26}} = \overline{Q_{62}} = mn^3 (Q_{11} - Q_{22} - 2Q_{66}) + m^3 n (Q_{12} - Q_{22} + 2Q_{66})$$

$$\overline{Q_{66}} = m^2 n^2 (Q_{11} + Q_{22} - 2Q_{12}) + (m^2 - n^2)^2 Q_{66} \tag{2.9}$$

2.3 Laminate Constitutive Equation

2.3.1 Strain-Displacement Relations

Since each lamina has individual coordinate system, the strain-displacement relation for a laminate is represented easily along a convenient common axis in the reference plane. The reference plane is selected along the mid-plane of the laminate for simplicity. Moreover, the laminae are assumed to be bending without slipping over each other and the cross-section of the laminate remains unwrapped. Transverse shear strain γ_{xz} and γ_{yz} are also considered to be negligible. Considering these assumptions the in-plane displacement at any point with coordinate *z* can be written as (see Figure 2.2)

$$u = u_o - z \frac{\partial w}{\partial x}$$

$$v = v_o - z\frac{\partial w}{\partial y}$$

$$w = w_o \tag{2.10}$$

where u_o, v_o and $w_o$are the displacements at reference plane in the x, y and z direction and are function of x and y only.

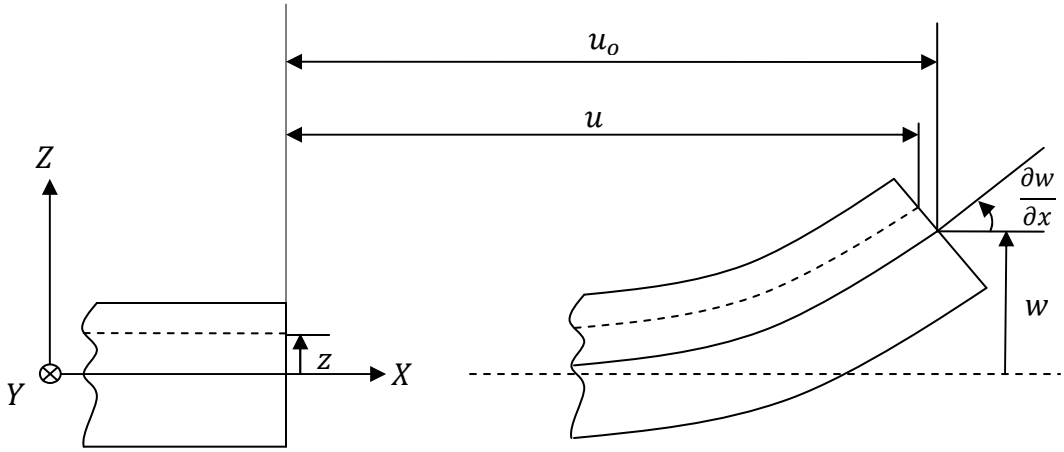

Figure 2.2 Laminate Section Before and After Deformation. [14]

The strain-displacement relation at any point can expressed as

$$\varepsilon_x = \frac{\partial u}{\partial x} = \frac{\partial u_o}{\partial x} - z\frac{\partial^2 w_o}{\partial x^2}$$

$$\varepsilon_y = \frac{\partial v}{\partial x} = \frac{\partial v_o}{\partial x} - z\frac{\partial^2 w_o}{\partial y^2}$$

$$\gamma_{xy} = \frac{\partial u}{\partial x} + \frac{\partial v}{\partial x} = \frac{\partial u_o}{\partial x} + \frac{\partial v_o}{\partial x} - 2z\frac{\partial^2 w_o}{\partial x \partial y}$$

(2.11)

In the matrix form Equations (2.11) can be also be written as

$$\begin{bmatrix} \varepsilon_x \\ \varepsilon_y \\ \gamma_{xy} \end{bmatrix} = \begin{bmatrix} \varepsilon_x^o \\ \varepsilon_y^o \\ \gamma_{xy}^o \end{bmatrix} + z \begin{bmatrix} \kappa_x \\ \kappa_y \\ \kappa_{xy} \end{bmatrix} \tag{2.12}$$

where,

$$\varepsilon_x^o = \frac{\partial u_o}{\partial x}$$

$$\varepsilon_y^o = \frac{\partial v_o}{\partial x}$$

$$\gamma_{xy}^o = \frac{\partial u_o}{\partial x} + \frac{\partial v_o}{\partial x}$$

(2.13A)

$$\kappa_x = -z\frac{\partial^2 w_o}{\partial x^2}$$

$$\kappa_y = -z\frac{\partial^2 w_o}{\partial y^2}$$

$$\kappa_{xy} = -2z\frac{\partial^2 w_o}{\partial x \partial y}$$

(2.13B)

2.3.2 Constitutive Equation of Laminated Plate

The stresses in the k^{th} ply at a distance of z_k from the reference plane in terms of strains and laminate curvatures can be expressed as

$$\begin{bmatrix} \sigma_x \\ \sigma_y \\ \tau_{12} \end{bmatrix}_{k^{th}} = \begin{bmatrix} \overline{Q_{11}} & \overline{Q_{12}} & \overline{Q_{16}} \\ \overline{Q_{21}} & \overline{Q_{22}} & \overline{Q_{26}} \\ \overline{Q_{61}} & \overline{Q_{62}} & \overline{Q_{66}} \end{bmatrix}_{k^{th}} \left\{ \begin{bmatrix} \varepsilon_x^o \\ \varepsilon_y^o \\ \gamma_{xy}^o \end{bmatrix} + z_k \begin{bmatrix} \kappa_x \\ \kappa_y \\ \kappa_{12} \end{bmatrix} \right\} \tag{2.14}$$

The strains in the laminate vary linearly through the thickness whereas the stresses very discontinuously. This is due to the different material properties of the layer resulting from different fiber orientation. Since there exists a discontinuous variation of stresses from a layer to

layer in the laminate, it is convenient to deal with system of equivalent forces and moments. The resultant forces and moments acting on the laminate can be defined as

$$N_x = \sum_{i=1}^{n} \int_{h_{k-1}}^{h_k} \sigma_x^k dz \qquad N_y = \sum_{i=1}^{n} \int_{h_{k-1}}^{h_k} \sigma_y^k dz \qquad N_{xy} = \sum_{i=1}^{n} \int_{h_{k-1}}^{h_k} \tau_{xy}^k dz$$

$$M_x = \sum_{i=1}^{n} \int_{h_{k-1}}^{h_k} \sigma_x^k z dz \qquad M_y = \sum_{i=1}^{n} \int_{h_{k-1}}^{h_k} \sigma_y^k z dz \qquad M_{xy} = \sum_{i=1}^{n} \int_{h_{k-1}}^{h_k} \tau_{xy}^k z dz$$

(2.15)

where N_x, N_y and N_{xy} are the forces per unit width of the beam M_x, M_y and M_{xy} are the moments per unit width of the beam, and t is the thickness of the beam. Substituting Equation (2.14) in Equation (2.15) the total constitutive equation or load-deformation relations for the laminate is as follows

$$\begin{bmatrix} N \\ M \end{bmatrix} = \begin{bmatrix} A & B \\ B & D \end{bmatrix} \begin{bmatrix} \varepsilon^0 \\ \kappa \end{bmatrix} \tag{2.16}$$

where

$$[A] = \sum_{k=1}^{n} [\bar{Q}]^k (h_k - h_{k-1})$$

$$[B] = \frac{1}{2} \sum_{k=1}^{n} [\bar{Q}]^k (h_k^2 - h_{k-1}^2)$$

$$[D] = \frac{1}{3} \sum_{k=1}^{n} [\bar{Q}]^k (h_k^3 - h_{k-1}^3)$$

(2.17)

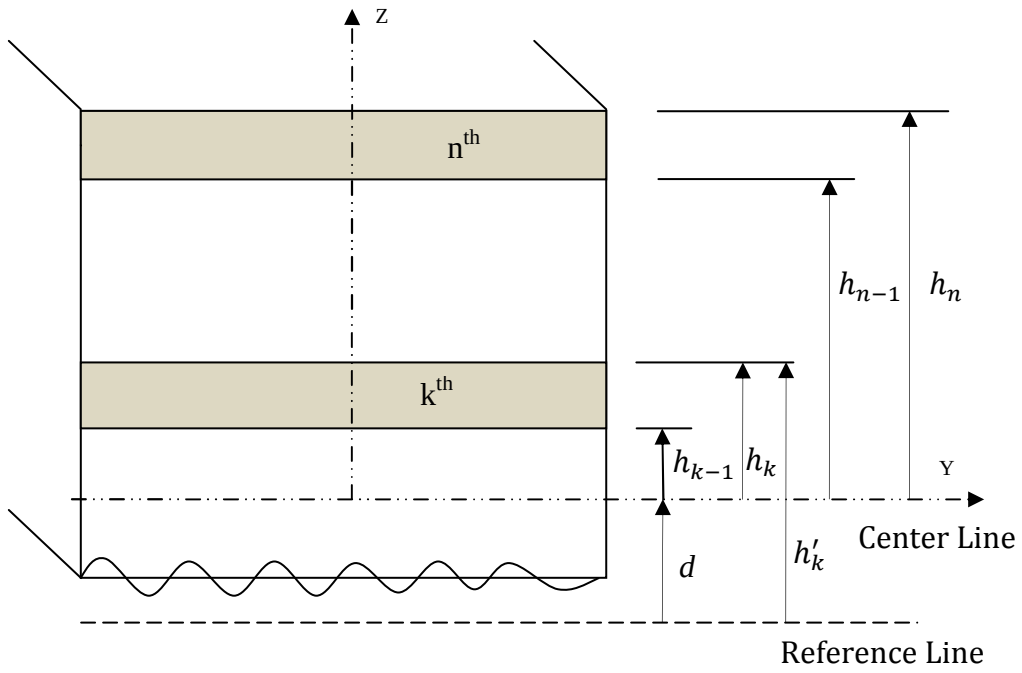

Figure 2.3 Coordinate Notations of Individual Plies.

h_k and h_{k-1} are the coordinates of the upper and lower surface of the kth lamina as shown in Figure 2. 3.

A matrix is called extensional stiffness matrix, B matrix is called the coupling stiffness matrix and D matrix is called the bending stiffness matrix. For a symmetrical laminate, it can be proved that B matrix is a zero matrix. For an unsymmetrical laminate B matrix is non-zero. Therefore, there exists coupling stiffness between in-plane and out-of plane.

The inverse of load-deformation relations is used to work easily with strains and curvature of the laminates for any applied load. Laminate compliance matrix can be expressed as

$$\begin{bmatrix} \varepsilon^0 \\ \kappa \end{bmatrix} = \begin{bmatrix} a & b \\ b^T & d \end{bmatrix} \begin{bmatrix} N \\ M \end{bmatrix} \tag{2.18}$$

where

$$\begin{bmatrix} a & b \\ b^T & d \end{bmatrix}_{6X6} = \begin{bmatrix} A & B \\ B & D \end{bmatrix}_{6X6}^{-1} \tag{2.19}$$

2.4 Translation of Laminate Axis for Laminated Beam

In the previous section, the laminate reference axis is selected at the mid-thickness of the laminate. In structural analysis, if the reference axis is not in the mid-thickness; the translation of the laminate axis is needed. Let d be the distance measuring from the new reference to the mid-thickness axis. Equation (2.17) can be rewritten as shown

$$[A'] = \sum_{k=1}^{n} [\bar{Q}]^k (h'_k - h'_{k-1}) = \sum_{k=1}^{n} [\bar{Q}]^k (h_k - h_{k-1}) = [A]$$

$$[B'] = \frac{1}{2} \sum_{k=1}^{n} [\bar{Q}]^k (h'^2_k - h'^2_{k-1}) = [B] + d[A]$$

$$[D'] = \frac{1}{3} \sum_{k=1}^{n} [\bar{Q}]^k (h'^3_k - h'^3_{k-1}) = [D] + 2d[B] + d^2[A] \tag{2.20}$$

where

$$h'_{k-1} = h_{k-1} + d \qquad\qquad h'_k = h_k + d \tag{2.21}$$

It should be noted that if a laminate is symmetrical with respect to its mid-axis (B=0) then the laminate becomes unsymmetrical as the reference axis is translated. However, the in-plane stiffness [A] remains the same.

2.5 Constitutive Equation for Laminated Composite Beam

2.5.1 Narrow and Wide Beams

The structural response of the beam is dependent on the ratio of the width to height of the beam cross section. For a beam subjected to bending, the induced lateral curvature is insignificant if the width to height ratio is large. This kind of beam is so-called “wide beam”.

Conversely, if the width to height ratio of the cross section is small, the beam is called “narrow beam”. For this case, the lateral curvature is induced due to the effect of Poisson’s ratio. As the result, lateral moment is zero.

In summary,

Wide beam, $M_y \neq 0$ $K_y = 0$

Narrow beam, $M_y = 0$ $K_y \neq 0$

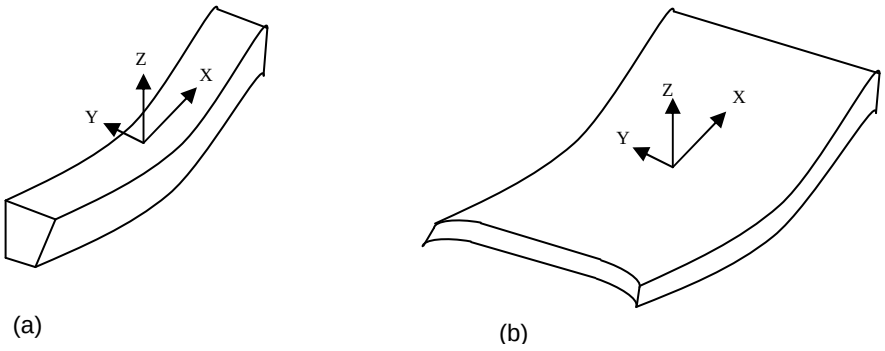

(a) (b)

Figure 2.4 (a) Narrow and (b) Wide Beams under Bending.

2.5.2 Constitutive Equation of Narrow Laminated Beam

For a narrow beam, there exists no force and moments in the y-direction. Hence, Equation (2.18) can be modified as

$$\begin{pmatrix} \varepsilon_x^o \\ K_x \end{pmatrix} = \begin{pmatrix} a_{11} & b_{11} \\ b_{11} & d_{11} \end{pmatrix} \begin{pmatrix} N_x \\ M_x \end{pmatrix} \tag{2.22}$$

Or

$$\begin{pmatrix} N_x \\ M_x \end{pmatrix} = \begin{pmatrix} A_1^* & B_1^* \\ B_1^* & D_1^* \end{pmatrix} \begin{pmatrix} \varepsilon_x^o \\ K_x \end{pmatrix} \tag{2.23}$$

Where,

$$A_1^* = \frac{1}{a_{11} - \frac{b_{11}^2}{d_{11}}}$$

$$B_1^* = \frac{1}{b_{11} - \frac{a_{11}d_{11}}{b_{11}}}$$

$$D_1^* = \frac{1}{d_{11} - \frac{b_{11}^2}{a_{11}}}$$

(2.24)

A_1^*, B_1^*, and D_1^* refer to the axial, coupling and bending stiffnesses of the beam

CHAPTER 3

APPROXIMATE CLOSED FORM SOLUTIONS OF COMPOSITE I-BEAM UNDER LOADING

This chapter describes the development of an analytical expression of sectional property calculation of composite laminated beam. The section properties include the centroid, the equivalent axial and bending stiffnesses of the section. The procedure to calculate stresses and strains of each layer in the flange and web laminates are also illustrated.

3.1 Geometry of Laminated I-Beam

The geometry of the laminated I-beam is depicted in Figure 3.1. I-section is divided into three sub-laminates, two flanges and a web. Their designated number is shown in the figure.

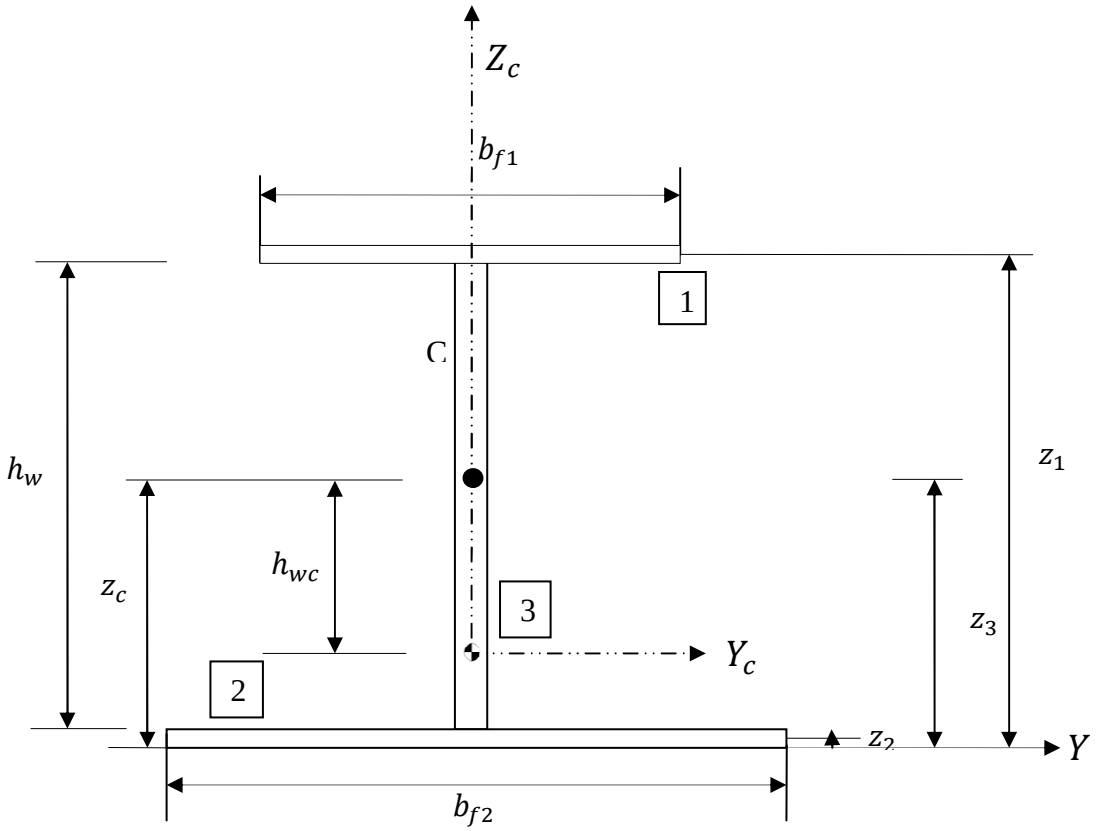

Figure 3.1 I-section Composite Beam with Unsymmetrical Flange Section.

3.2 Centroid of Composite I-Beam

The centroid of a structural cross-section is defined here as the average location of forces acting on each part of the cross section. To calculate this location, we first set the Y-axis aligned to the bottom surface of the lower flange and because of its symmetry with respect to middle line of the width the Z-axis is aligned at the this line. The distances between the Y-axis and the mid-plane of the flange and the web laminates are specified as shown in Figure 3.1. The net force acting on the centroid is given as

$$\overline{N_x} z_c = b_{f1} N_{x1} z_1 + b_{f2} N_{x2} z_2 + h_w N_{x3} z_3 \tag{3.1}$$

where

$$\overline{N_x} = b_{f1} N_{x1} + b_{f2} N_{x2} + h_w N_{x3} \tag{3.2}$$

N_{x1}, N_{x2}, and N_{x3} are the axial forces per unit width of sub-laminates 1, 2, and 3 along X direction. $\overline{N_x}$ is the total force acting on I-section in the X direction.

Therefore, the centroid of I-section can be calculated as

$$z_c = \frac{b_{f1} A^*_{1,f1} z_1 + b_{f2} A^*_{1,f2} z_2 + h_w A^*_{1,f3} z_3}{b_{f1} A^*_{1,f1} + b_{f2} A^*_{1,f2} + h_w A^*_{1,f3}} \tag{3.3}$$

where A^*_1 is defined in Eqn 2.24 for each sub-laminates and z_c is the distance between the Y-axis and the centroid.

3.3 Equivalent Axial Stiffness, $\overline{EA}$

3.3.1 Constitutive Equation for Sub-laminates

From the constitutive equation of narrow laminated beam (See Eqns 2.23 and 2.24), the constitutive equation for sub-laminates can be deduced as

For sub-laminate 1 (top flange laminate)

$$N_{x1} = A^*_{1,f1} \varepsilon^o_{x,f1} + B^*_{1,f1} K_{x,f1} \tag{3.4}$$

$$M_{x1} = B^*_{1,f1} \varepsilon^o_{x,f1} + D^*_{1,f1} K_{x,f1} \tag{3.5}$$

For sub-laminate 2 (bottom flange laminate)

$$N_{x2} = A^*_{1,f2}\varepsilon^o_{x,f2} + B^*_{1,f2}K_{x,f2} \tag{3.6}$$

$$M_{x2} = B^*_{1,f2}\varepsilon^o_{x,f2} + D^*_{1,f2}K_{x,f2} \tag{3.7}$$

However, for the web laminate,

$$K_{x,w} = 0$$

Therefore, it can be deduced for web laminate as

$$N_{x,w} = A^*_{1,w}\varepsilon^o_{x,w} \tag{3.8}$$

$$M_{x,w} = B^*_{1,w}\varepsilon^o_{x,w} \tag{3.9}$$

3.3.2 Analytical Expression for Equivalent Axial Stiffness, $\overline{EA}$

The axial force is applied at the centroid to develop an expression for equivalent axial stiffness, $\overline{EA}$. The total force in the X-direction can be written as

$$\overline{N_x} = \overline{EA}\ \varepsilon^c_x \tag{3.10}$$

where, $\overline{EA}$ is the equivalent axial stiffness of the entire cross-section.

Substituting Equations 3.4 through 3.9 in Equation. 3.2, we get

$$\overline{N_x} = b_{f1}\left(A^*_{1,f1}\varepsilon^o_{x,f1} + B^*_{1,f1}K_{x,f1}\right) + b_{f2}\left(A^*_{1h,f2}\varepsilon^o_{x,f2} + B^*_{1,f2}K_{x,f2}\right) + h_w\left(A^*_{1,w}\varepsilon^o_{x,w}\right) \tag{3.11}$$

Since the strain for all laminates are equal along the x-axis, we have

$$\varepsilon^o_{x,f1} = \varepsilon^o_{x,f2} = \varepsilon^o_{x,w} = \varepsilon^c_x \tag{3.12}$$

where, ε^c_x is the strain at the centroid in the x-direction.

Moreover, no radius of curvature exists for all laminates because of load at the centroid of the entire cross-section.

This implies

$$K_{x,f1} = K_{x,f2} = K_{x,w} = 0 \tag{3.13}$$

Therefore, Equation 3.5 can be written as

$$\overline{N_x} = \{b_{f1}(A^*_{1,f1}) + b_{f2}(A^*_{1h,f2}) + h_w(A^*_{1,w})\}\varepsilon^c_x \quad (3.14)$$

Comparing with Equation 3.4 and 3.8, equivalent axial stiffness can be calculated as

$$\overline{EA} = \{b_{f1}(A^*_{1,f1}) + b_{f2}(A^*_{1h,f2}) + h_w(A^*_{1,w})\} \quad (3.15)$$

3.3.3 Stresses and Strains in Layers of Flange Laminates using Equivalent Axial Stiffness, $\overline{EA}$

The stress and strain of any given layer in flanges laminates can found by finding mid-plane strain and radius of curvature for laminates.

Consider a load, P acting at the centroid, such that the equivalent axial stiffness is calculated as per the method in previous section.

Therefore,

$$P = \overline{N_x} = \overline{EA}\varepsilon^c_x \qquad \text{and} \qquad \overline{M_x} = 0 \quad (3.16)$$

$$\begin{bmatrix}\overline{N_x}\\ \overline{M_x}\end{bmatrix} = \begin{bmatrix}\overline{EA} & 0\\ 0 & D^c_x\end{bmatrix}\begin{bmatrix}\varepsilon^c_x\\ K^c_x\end{bmatrix} \quad (3.17)$$

Hence

$$\varepsilon^c_x = \frac{P}{\overline{EA}} \text{ and } K^c_x = 0 \quad (3.18)$$

For sub-laminates 1,

$$\varepsilon^o_{x,f1} = \varepsilon^c_x$$

$$K_{x,f1} = 0$$

From Equations 3.4 & 3.5, force and moment per unit width of sub-laminate 1 are

$$N_{x1} = A^*_{1,f1}\varepsilon^c_x \quad (3.19)$$

$$M_{x1} = B^*_{1,f1}\varepsilon^c_x \quad (3.20)$$

The mid-plane strain and radius of curvature for flange laminate can be found from the above equations

In matrix form

$$\begin{pmatrix} \varepsilon^{o}_{x,f1} \\ \varepsilon^{o}_{y,f1} \\ \gamma^{o}_{xy,f1} \\ K_{x,f1} \\ K_{y,f1} \\ K_{xy,f1} \end{pmatrix} = \begin{pmatrix} a_{11} & b_{11} & b_{16} \\ a_{12} & b_{21} & b_{26} \\ a_{16} & b_{61} & b_{66} \\ b_{11} & d_{11} & d_{16} \\ b_{12} & d_{12} & d_{26} \\ b_{16} & d_{61} & d_{66} \end{pmatrix}_1 \begin{pmatrix} N_{x1} \\ M_{x1} \\ M_{xy1} \end{pmatrix} \tag{3.21}$$

Where

$$M_{xy1} = -\frac{1}{d_{66}}[(b_{16})_1 . N_{x1} + (d_{61})_1 . M_{x1}]$$

Since

$$K_{xy1} = 0$$

From mid-strain data the strain in flange sub-laminate 1 can be calculated as

$$\left[\varepsilon_{fl}\right]_k = [\varepsilon^o]_{fl} + z_{k1} . [K]_{fl} \tag{3.22}$$

where z_{k1} is the position of kth layer from the mid-plane of sub-laminate 1 (top flange)

Expanding

$$\begin{pmatrix} \varepsilon_{x,f1} \\ \varepsilon_{y,f1} \\ \varepsilon_{xy,f1} \end{pmatrix}_{k1} = \begin{pmatrix} \varepsilon^{o}_{x,f1} \\ \varepsilon^{o}_{y,f1} \\ \gamma^{o}_{xy,f1} \end{pmatrix} + z_{k1} . \begin{pmatrix} K_{x,f1} \\ K_{y,f1} \\ K_{xy,f1} \end{pmatrix}_1 \tag{3.23}$$

Using lamination theory, stress in k^{th} layer is calculated as

$$\left[\sigma_{fl}\right]_k = [\bar{Q}]_{k1} . \left[\varepsilon_{fl}\right]_k \tag{3.24}$$

Similarly, above method can be followed to find stress and strain in sub-laminate 2 (bottom flange).

3.3.4 Stresses in Web Laminate using Equivalent Axial Stiffness, $\overline{EA}$

For the web laminate under axial loading

$$K_{x,w} = 0$$

Therefore

$$\varepsilon^o_{x,w} = \varepsilon^c_x = \frac{P}{\overline{EA}} \tag{3.25}$$

The force and moment in laminate are

$$N_{x,w} = A^*_{1,w}\varepsilon^o_{x,w}$$

$$M_{x,w} = B^*_{1,w}\varepsilon^o_{x,w}$$

If the web laminate is symmetrical, then $\mathrm{B}^*_{1,\mathrm{w}}$ is zero

Hence

$$M_{x,w} = 0$$

The stress and strain in different layers of the web laminate can be calculated using the Equation (3.15) through Equation (3.18).

3.4 Equivalent Bending Stiffness, D^c_x

3.4.1 Analytical Expression for Equivalent Bending Stiffness, D^c_x

A moment is applied at the centroid to develop an expression for the equivalent bending stiffness, Dx. The total moment applied in the X-direction can written as

$$\overline{M_x} = D^c_x K^c_x \tag{3.26}$$

or

$$\overline{M_x} = b_{f1}M_{x1} + b_{f1}N_{x1}z_{1c} + b_{f2}M_{x2} + b_{f2}N_{x2}z_{2c} + \int_{-\left(\frac{h_w}{2}-h_{wc}\right)}^{\frac{h_w}{2}+h_{wc}} z\,N_{x,w}dz \tag{3.27}$$

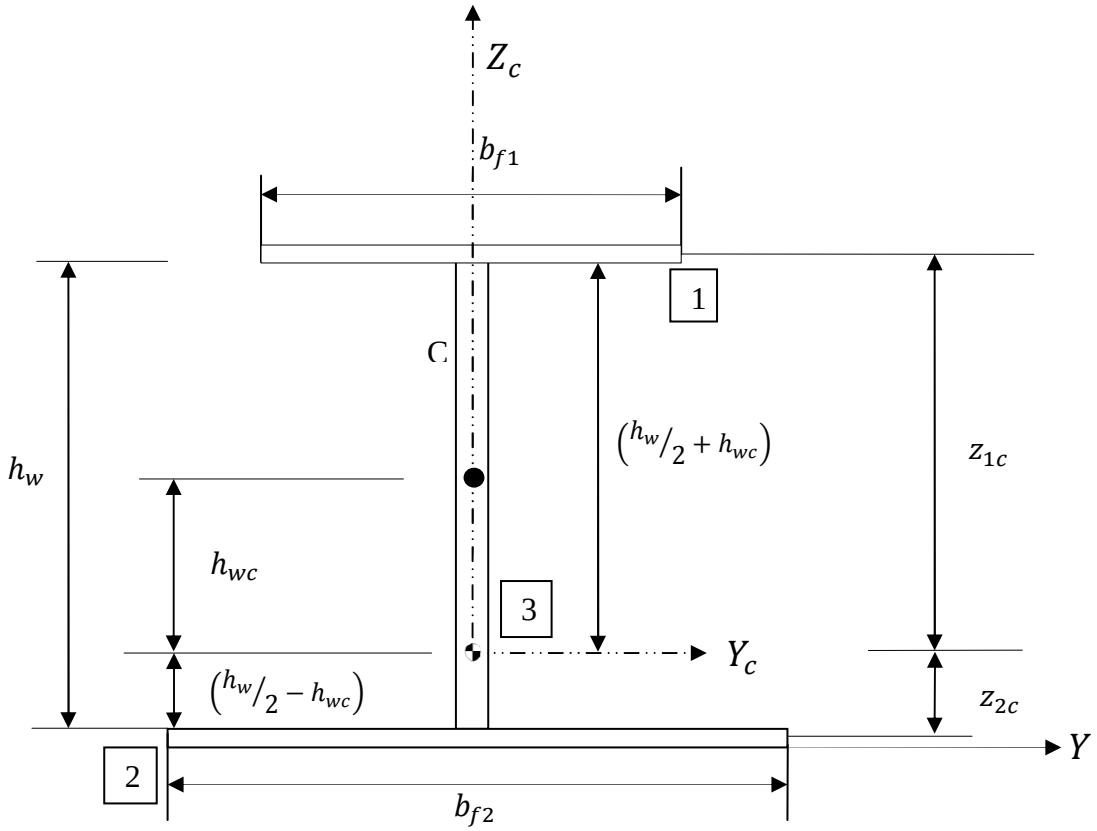

Figure 3.2 Distances between Mid-planes of Sub-laminates from Centroid.

From the above equation, for sub-laminate 1

$$b_{f1}M_{x1} + b_{f1}N_{x1}z_{1c} = b_{f1}\left(B^*_{1,f1}\varepsilon^o_{x,f1} + D^*_{1,f1}K_{x,f1}\right) + b_{f1}\left(A^*_{1,f1}\varepsilon^o_{x,f1} + B^*_{1,f1}K_{x,f1}\right)z_{1c}$$

Here,

$$K_{x,f1} = K^c_x$$

$$\varepsilon^o_{x,f1} = \varepsilon^c_x + z_{1c}K_{x,f1} \tag{3.28}$$

But

$$\varepsilon^c_x = 0$$

Therefore

$$b_{f1}M_{x1} + b_{f1}N_{x1}z_{1c} = b_{f1}\left(A^*_{1,f1}z^2_{1c} + 2B^*_{1,f1}z_{1c} + D^*_{1,f1}\right)K^c_x \tag{3.29}$$

Similarly for sub-laminate 2,

$$b_{f2}M_{x2} + b_{f2}N_{x2}z_{2c} = b_{f2}\left(A^*_{1,f2}z^2_{2c} + 2B^*_{1,f2}z_{2c} + D^*_{1,f2}\right)K^c_x \tag{3.30}$$

For sub-laminate 3 (web laminate)

$$\overline{M_w} = \int_{-\left(\frac{h_w}{2}-h_{wc}\right)}^{\frac{h_w}{2}+h_{wc}} z\, N_{x,w}\, dz \tag{3.31}$$

where,

$$N_{x,w} = A^*_{1,w}\varepsilon^o_{x,w} = A^*_{1,w}\left(\varepsilon^c_x + zK^c_{x,w}\right) \tag{3.32}$$

From Equation 3.7,

$$N_{x,w} = A^*_{1,w}zK^c_{x,w} \tag{3.33}$$

Therefore

$$\int_{-\left(\frac{h_w}{2}-h_{wc}\right)}^{\frac{h_w}{2}+h_{wc}} z\, N_{x,w}\, dz = \int_{-\left(\frac{h_w}{2}-h_{wc}\right)}^{\frac{h_w}{2}+h_{wc}} z\, A^*_{1,w}zK^c_x\, dz \tag{3.34}$$

$$\int_{-\left(\frac{h_w}{2}-h_{wc}\right)}^{\frac{h_w}{2}+h_{wc}} z\, N_{x,w}\, dz = A^*_{1,w}\left(\frac{1}{12}h^3_w + h_w h^2_{wc}\right)K^c_x \tag{3.35}$$

By substituting back into moment equation

$$\overline{M_x} = \left\{ \begin{matrix} b_{f1}\left(A^*_{1,f1} z^2_{1c} + 2B^*_{1,f1} z_{1c} + D^*_{1,f1}\right) \\ +b_{f2}\left(A^*_{1,f2} z^2_{2c} + 2B^*_{1,f2} z_{2c} + D^*_{1,f2}\right) \\ +A^*_{1,w}\left(\frac{1}{12} h^3_w + h_w h^2_{wc}\right) \end{matrix} \right\} K^c_x \quad (3.36)$$

By comparing with Equation (3.20), the equivalent bending stiffness can be written as

$$D^c_x = \left\{ \begin{matrix} b_{f1}\left(A^*_{1,f1} z^2_{1c} + 2B^*_{1,f1} z_{1c} + D^*_{1,f1}\right) + b_{f2}\left(A^*_{1,f2} z^2_{2c} + 2B^*_{1,f2} z_{2c} + D^*_{1,f2}\right) \\ +A^*_{1,w}\left(\frac{1}{12} h^3_w + h_w h^2_{wc}\right) \end{matrix} \right\}$$

(3.37)

3.4.2 Stresses and Strains in Layers of Flange Laminate using Equivalent Bending Stiffness, D^c_x

Same approach of finding mid-plane strain and curvature and then using lamination theory equations is followed to find stresses in the layers.

A moment load is considered acting at the centroid such that the equivalent bending stiffness is calculated as per the method above.

Therefore,

$$\overline{M_x} = D^c_x K^c_x \quad \text{and} \quad \overline{N_x} = 0$$

or

$$K^c_x = \frac{\overline{M_x}}{D^c_x} \quad (3.38)$$

Moreover,

$$\varepsilon^c_x = 0$$

$$K_{x,f1} = K^c_x$$

Hence for the sub-laminate 1

$$\varepsilon^o_{x,f1} = \varepsilon^c_x + K_{x,f1} z_{1c} = K^c_x z_{1c} \quad (3.39)$$

$$N_{x1} = A^*_{1,f1} \varepsilon^o_{x,f1} + B^*_{1,f1} K_{x,f1} = \left(A^*_{1,f1} z_{1c} + B^*_{1,f1}\right) K^c_x = \left(A^*_{1,f1} z_{1c} + B^*_{1,f1}\right) \frac{\overline{M_x}}{D^c_x}$$

(3.40)

$$M_{x1} = B^*_{1,f1}\varepsilon^o_{x,f1} + D^*_{1,f1}K_{x,f1} = \left(B^*_{1,f1}z_{1c} + D^*_{1,f1}\right)K^c_x = \left(B^*_{1,f1}z_{1c} + D^*_{1,f1}\right)\frac{\overline{M_x}}{D^c_x}$$

(3.41)

The stress and strain in layers of flange laminate can be calculated using Equation (3.15) through Equation (3.18).

Similarly, the above method can be followed to find stress and strain in Sub-laminate 2 (bottom flange).

3.4.3 Stresses in Web Laminate using Equivalent Bending Stiffness, D^c_x.

For the web laminate under bending, we have

$$K^c_x = K^c_{x,w} = \frac{\overline{M_x}}{D^c_x} \qquad \text{and} \qquad \varepsilon^c_x = 0 \tag{3.42}$$

The force and moment in the web-laminate is

$$N_{x,w} = A^*_{1,w}\varepsilon^o_{x,w} = A^*_{1,w}K^c_x z$$

$$M_{x,w} = B^*_{1,w}\varepsilon^o_{x,w} = B^*_{1,w}K^c_x.z$$

(3.43)

Since the web laminate is always symmetrical, then $\mathrm{B}^*_{1,\mathrm{w}}$ is zero

Hence

$$M_{x,w} = 0$$

The stress and strain in different layers of the web the laminate can be calculated using Equation (3.15) through Equation (3.18).

CHAPTER 4

FINITE ELEMENT MODELING AND VALIDATION

A 3-D finite element model of a composite I-section beam is developed to validate the analytical expression developed for calculating sectional property as described in Chapter 3. ANSYS 11.0 Classic is used to develop the required 3-D finite element model. This chapter explains in detail the geometry and material property of laminated composite material, step vise procedure to develop the composite finite element model, and the boundary and loading conditions applied on the model. The finite element model is developed in such a way to eliminate the smear effect of the properties in the composite laminate beam.

4.1 Geometry and Material Properties of Composite Laminate

4.1.1 Material Properties

The material used for the composite laminate is T300/977-2 graphite/epoxy laminate. The unidirectional layer orthotropic properties for the material are given as

$$E_1 = 21.75 \text{ X } 10^6 \text{ psi}, \quad E_2 = 1.595 \text{ X } 10^6 \text{psi}, \quad E_3 = 1.595 \text{ X } 10^6 \text{psi}$$

$$\nu_{12} = 0.25, \qquad \nu_{23} = 0.25, \qquad \nu_{23} = 0.25,$$

$$G_{12} = 0.8702 \text{ X } 10^6 \text{ psi}, \quad G_{23} = 0.5366 \text{ X } 10^6 \text{ psi}, \quad G_{13} = 0.8702 \text{ X } 10^6 \text{ psi}$$

where E_1, E_2, and E_3 are the Young's moduli of the composite lamina along the material coordinates. G_{12},G_{23}, and $G_{13}$are the Shear moduli and ν_{12}, ν_{23}, and ν_{13} are Poisson's ratio with respect to the 1-2, 2-3 and 1-3 planes, respectively.

4.1.2 Geometry of Finite Element Model.

The I-section composite model considered here includes symmetrical and unsymmetrical flanges with top and bottom flanges consisting of 8 and 10 layers, respectively, with ply thickness of 0.005'' each. The web used is of the width 0.5'' and consists of 4 layers. The stacking sequence for web laminate is $[\pm 45]_s$. Whereas for top and bottom flanges the stacking sequence is $[\pm 45/90/0]_s$ and $[\pm 45/0_2/90]_s$, respectively. Three cases of flange lengths are considered for parametric study. The dimension of the top and bottom flanges can be seen in Table 4.1.

Table 4.1 Dimension of Flanges for Different Cases

CASE	Width of top flange (in)	Width of bottom flange (in)	Height of Web (in)
1	0.25	1	0.5
2	0.5	0.75	0.5
3	0.625	0.625	0.5

4.2 Development of Finite Element Model

ANSYS 11.0 classic has been used to develop the finite element model. 3-D 8 nodes SOLID45 elements are used to develop the required 3D composite model. A simpler element is chosen to make model simpler and thus reducing the computation time. However, choice of the element over higher order element doesn't comprise the accuracy, as the choice is based on test of SOLID45 for basic and simple problems involving ability of the element to capture transverse shear effect in deflection. In the 3-D composite model of I-beam, each layer in the laminate is mapped meshed separately in thickness direction with different element coordinate system to represent a composite layer arrangement. A layer by layer arrangement is adopted

to create a model, instead of convectional composite modeling technique of using SOLID46 element. This method is adopted to avoid the limitation in modeling a composite laminate in ANSYS. The SOLID46 element is 3-D 8 nodes layered element which assumes smearing of the composite laminate material property to solve the problem. The closed form solution for sectional properties in Chapter 3 are derived based on non-smearing of material property.

4.2.1 Modeling and Mesh Generation

The following procedure is used to create the 3-D finite element model and generate mesh.

1. 2D 4 nodes PLANE42 and 3D 8 nodes SOLID45 elements are defined as element type 1 and element type 2, respectively. Unidirectional orthotropic material properties for lamina are defined in material property section.
2. The I-section beam is modeled sequentially in 3 parts. First, the top flange is modeled, and then the web section, and finally the bottom flange are modeled. Each laminate is modeled layer by layer.
3. Initially, a 2D base area for laminate 1 is modeled in the XY plane at Z=0. This is done by creating various keypoints according to the dimension of the laminate. The area is plotted through the keypoints. This can be seen in Figure 4.1 below.

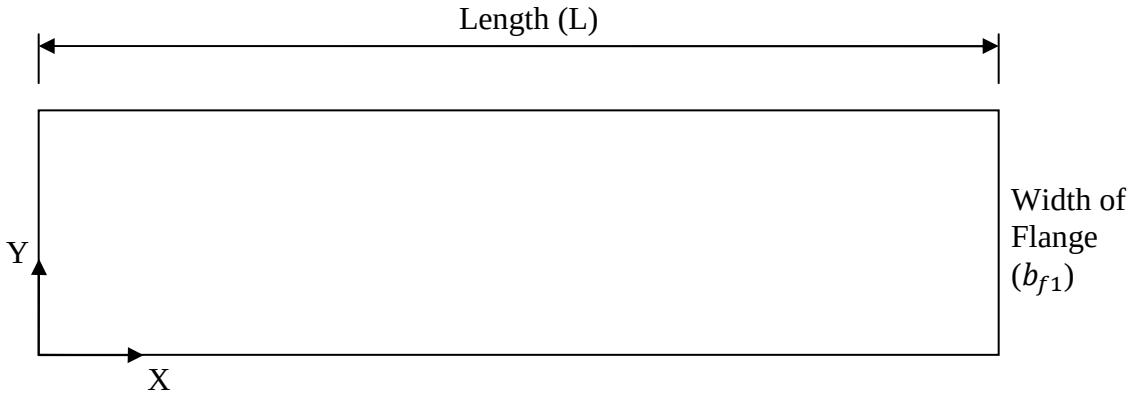

Figure 4.1 2D Area Dimensions for Sub-laminate 1.

4. To create a 2D mesh on the area, the lines are selected and the number of division required for mapped meshing is specified. The size of the element along the width of the area is maintained as per thickness of layer i.e. 0.005”. The spacing ratio for the line divisions is given negative to increase the density of the elements at the ends of the beam. This is done because the loads for the beam are applied at the ends for all analysis and also to reduce the number of elements for quicker computation.
5. The area is mapped meshed using PLANE42 elements. After mapped meshing the area, the 2D element mesh generated in the XY plane at Z=0 can be seen as in Figure 4.2.

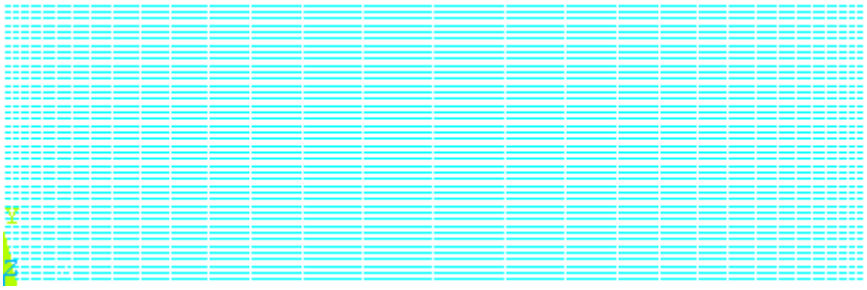

Figure 4.2 2D Area Mesh Generated using PLANE42 Elements.

6. 8 element coordinate system is created, corresponding to each fiber orientation of each layer in the composite laminate. Then again, the coordinate system is reset to global coordinate system.
7. To create a 3D mesh for the first layer of top laminate from the bottom, corresponding element coordinates system is selected. The element type is set as SOLID45, and then area created with 2D elements at Z=0 is extruded in the Z direction for a thickness of 0.005”. A 3D mesh of tetrahedron elements representing first layer is generated by deleting the 2D area mesh.
8. The second layer in the Sub-laminate 1 is created by selecting the corresponding element coordinate system and SOLID45 element, and then extruding the top area of layer 1 in the XY plane through the Z direction for thickness of 0.005”.

9. Same procedure is followed to generate other layer in the laminate by choosing the corresponding element coordinate system. After extruding all layer of Sub-laminate 1, the meshing can be seen as in Figure 4.3
10. For web section, the first layer is created by creating a volume as per dimension and then meshing it. This is done by creating a local coordinate system such that the keypoints of the area (with length and width as dimensions) is created in XY plane and extruded in Z axis through the thickness of 0.005". This method is opted to create web section instead of the method explained above because; a 2D area mesh for the area cannot be created with PLANE42 elements in global the XZ plane. The volume created for the web laminate can be seen in Figure 4.4.

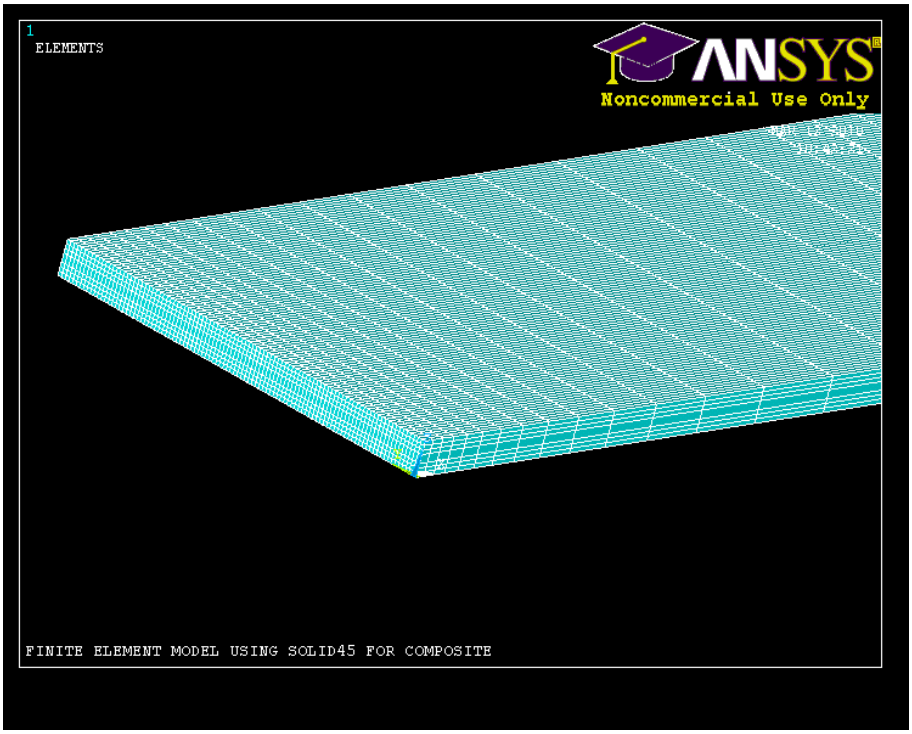

Figure 4.3 Mapped Meshing of Sub-laminate 1 (top flange).

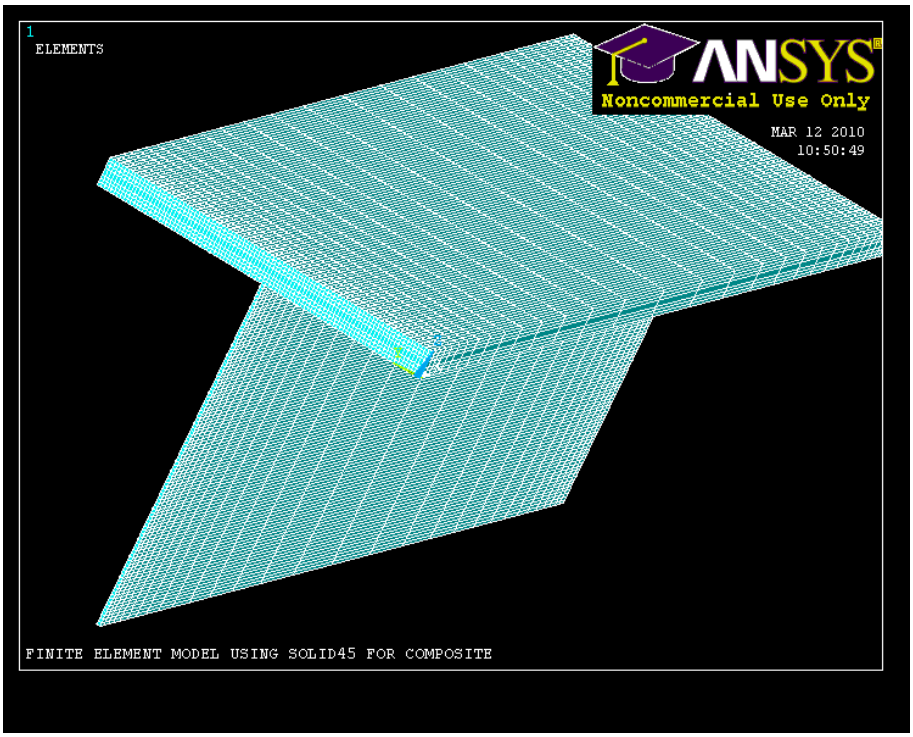

Figure 4.4 Mapped Meshing of First Layer of Sub-laminate 3.

11. 4 element coordinate systems corresponding to each fiber orientation for each layer in the composite web laminate are defined. The element coordinates are defined relative to the local coordinate system used to create the volume for the first layer. This ensures that the elements in the layers of the web laminate make orientation with respect to the XY plane of the local coordinate system.
12. The lines representing the length are selected and number divisions for the mapped mesh is specified. The number of division and spacing ratio in the lines is given same as the numbers for the lines in the area created for Sub-laminate 1. The other lines in the volume are selected and number of divisions for the mapped mesh is specified as the thickness of the layers i.e. 0.005”. This is to ensure proper sizing of elements for merging of nodes.
13. To create a 3D mapped mesh for the first layer, corresponding element coordinate system is selected and element type is set as SOLID45. The volume in mapped meshed to create 3D mesh of hexahedron elements.

14. The next layer in web laminate is created by selecting corresponding element coordinate system and extruding the area at Z=0.005” in the XY plane of local coordinate system. The other layers in the web are modeled in the similar way to complete the web section.
15. Finally, the Sub-laminate 2 (bottom flange) is modeled using method similar to the method used to model Sub-laminate 1. To begin, a local coordinate system is defined to represent the local coordinate system for Sub-laminate 2.

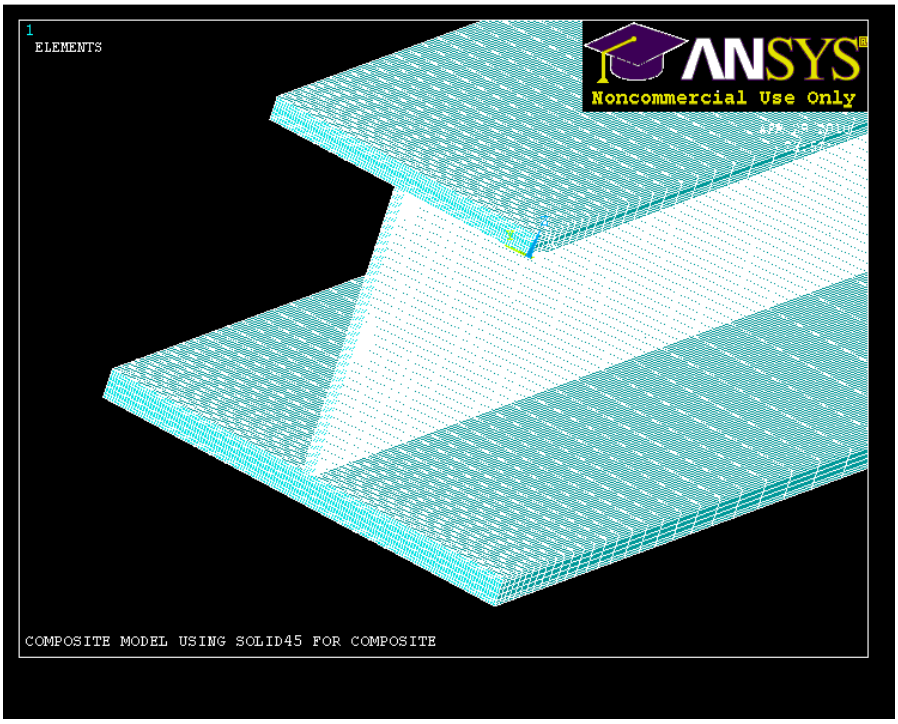

Figure 4.5 Final Finite Element Model.

16. All the nodes and keypoints are merged for adjacent layers faces, which are in contact with each other. The element sizing and spacing ratio of the elements is of primary importance for proper merging. The proper merging between layers ensures bonding between them and continuity of the finite element model. With merging desired finite model is complete. The final finite element model can be seen in Figure 4.5.

4.2.2 Boundary and Loading Condition

The following boundary conditions are applied for the model. Since the finite element model is used to analyze the cantilever beam condition, all the nodes at X=0 plane is selected and deflection is all direction is set to zero i.e. U_x=0; U_y=0; U_z=0.

4.3 Validation of Finite Element Model

The finite element model is validated using isotropic properties while maintaining model size, element orientation and boundary conditions same. The I-beam with 0.5" and 0.75" width of the top and bottom flanges and 0.5" height of the web laminate (Case 2 I-beam section) was used to validate the model. The isotropic property used for validation is as follows

$$E_1 = E_2 = E_3 = 1.02 \text{ X } 10^7 \text{ psi}$$

$$\nu_{12} = \nu_{23} = \nu_{23} = 0.25$$

$$G_{12} = G_{23} = G_{13} = \frac{E_{11}}{2(1+\nu_{12})} = 4.06 \text{ X } 10^6 \text{ psi}$$

Since the deflection for cantilever beam including its transverse shear deflection at its free end is well defined, the finite element model is validated using the same condition.

Since the theory used to calculate the end deflection defines the deflection of the beam at its cross section centroid. For a beam of length of 'L' and tip load of 'P', the deflection at the free end can be written as

$$\delta_b = \frac{PL^3}{3EI}$$

And transverse shear deflection can be written as [16]

$$\delta_s = f_s \frac{PL}{GA}$$

Where f_s is termed as form factor of shear, and for I-section it is given as

$$f_s = \frac{A}{A_{web}}$$

The finite element deflection is determined at the centroid of the I-section. Comparison of the results obtained by analytical method and FEM can be seen in Table 4.2

Table 4.2 Comparison of Analytical and Finite Element Solution for Isotropic Material

Length, L	load, P	Analytical Solution			FEM	**DEFL. ERROR %**
(in)	(lb)	Lateral deflection $\delta_b = \frac{PL^3}{3EI}$ (in)	Deflection due to Transverse shear $\delta_s = f_s \frac{PL}{GA}$ (in)	Total deflection $\delta_b + \delta_s$ (in)	(in)	
5	200	1.966E-01	2.463E-02	2.213E-01	2.187E-01	**.114E+01**
6	200	3.398E-01	2.956E-02	3.693E-01	3.663E-01	**.821E+00**
7	200	5.395E-01	3.448E-02	5.740E-01	5.706E-01	**.596E+00**
8	200	8.054E-01	3.941E-02	8.448E-01	8.410E-01	**.445E+00**
9	200	1.147E+00	4.433E-02	1.191E+00	1.187E+00	**.342E+00**
10	200	1.573E+00	4.926E-02	1.622E+00	1.618E+00	**.265E+00**

As indicated in the table, deflection difference between the FEM and exact solution is very small. With this mind, we can further apply the model to the composite property.

CHAPTER 5

RESULTS FOR CLOSED FORM EXPRESSIONS

This chapter explains in detail the validation results for the analytical expression derived in Chapter 2. It also compares and analysis the 3 cases of I-section beam under loading. Finally the stresses along principal axis in the layers on the beam is calculated and analyzed.

5.1 Results Comparison of Centroid Calculation

In this study, the centroid calculation derived in Chapter 2 is validated using the finite element solution. For the validation, isotropic material properties are chosen as

$$E_1 = E_2 = E_3 = 1.02 \text{ X } 10^7 \text{ psi}$$

$$\nu_{12} = \nu_{23} = \nu_{23} = 0.25$$

$$G_{12} = G_{23} = G_{13} = \frac{E_{11}}{2(1+\nu_{12})} = 4.06 \text{ X } 10^6 \text{ psi}$$

After this, composite material is used. The material property of composite materials used is

$$E_1 = 21.75\ X\ 10^6 \text{ psi}, \quad E_2 = 1.595\ X\ 10^6 \text{ psi}, \quad E_3 = 1.595\ X\ 10^6 \text{ psi}$$

$$\nu_{12} = 0.25, \qquad \nu_{23} = 0.45, \qquad \nu_{13} = 0.25,$$

$$G_{12} = 0.8702\ X\ 10^6 \text{ psi}, \quad G_{23} = 0.5366\ X\ 10^6 \text{ psi}, \quad G_{13} = 0.8702\ X\ 10^6 \text{ psi}$$

5.1.1 Isotropic Material

The centroid of I-section can be calculated easily, therefore by using isotropic material property the centroid expression derived for composite material can be validated. Centroid of an I-section can be calculated using mechanics approach as

$$z_c = \frac{\sum_i^n A_i Z_i}{\sum_i^n A_i} \tag{5.1}$$

where n is the number divisions of area used to represent the I-section

Table 5.1 lists the results of the centroid calculated using two methods for cases 1, 2 and 3. The results show an excellent agreement with each other.

Table 5.1 Results for Centroid of I-Section for Isotropic Material

	Case	Mechanics approach	Present Method	% Difference
		Eq. 5.1	Eq. 3.3	
z_c (in)	1	0.1421	0.1421	0.0
	2	0.2272	0.2272	0.0
	3	0.2721	0.2721	0.0

5.1.2 Composite Material

For composite materials, the centroid of the I-section depends on the fiber orientation and sequence of the layer. The centroid of the section moves between the top and bottom flange depending on the stiffness of the sub-laminates. With the increase in stiffness of the bottom flange the centroid moves closer towards bottom flange. Table 5.2 shows the centroid for various I-sections. The variation of the centroid for various I-section are plotted in Figure 5.1

Table 5.2 Results for Centroid of I-Section for Composite Material

	Case	Present Method
		Eq. 3.3
z_c (in)	1	0.1177
	2	0.1976
	3	0.2424

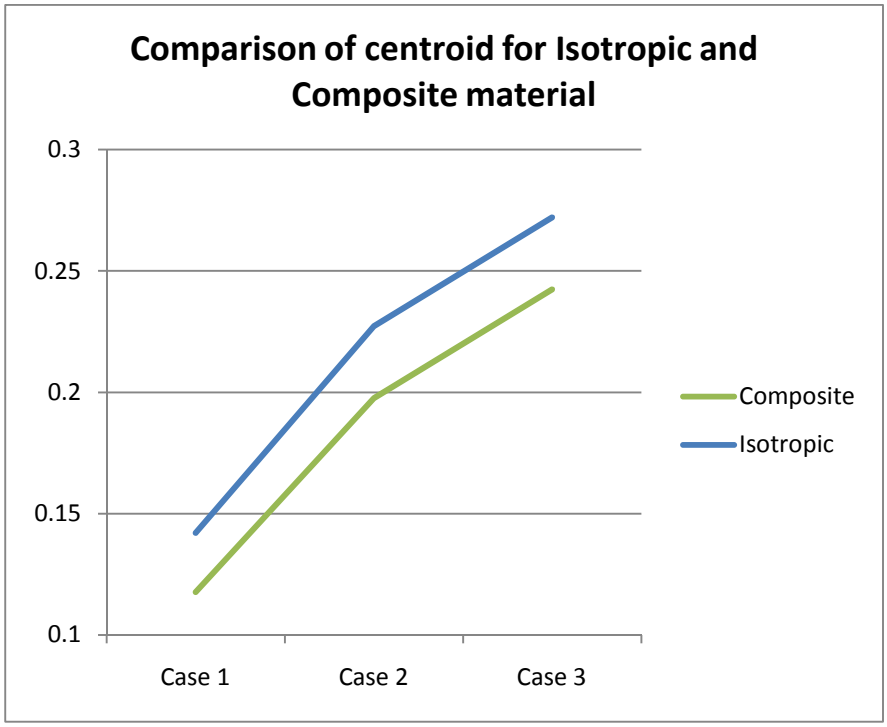

Figure 5.1 Variation of the Centroid along the Z-axis for Different Cases

5.2 Results Comparison for I-Beam Stiffness

The axial and bending stiffnesses of isotropic I-beam are known; therefore the expression for axial and bending stiffness can be validated by comparing the solution from finite element model. Two cases of loading were applied to the finite element model to calculate axial and bending stiffness. An axial load of 200lb was applied at the centroid of the cross-section as shown in Figure 5.2. The meshing of I-beam was done with extreme care so that a node is always present at the centroid of the cross-section.

For determining bending stiffness, a pair of forces with the same magnitude but opposite sign is applied to generate the moment at the centroid; a force of 100lb is applied one ply away from the centroid of the cross-section. This pair of forces generates a total moment of 0.5 lb-in about the x axis. The pair of force applied on finite element model is shown in Figure 5.3

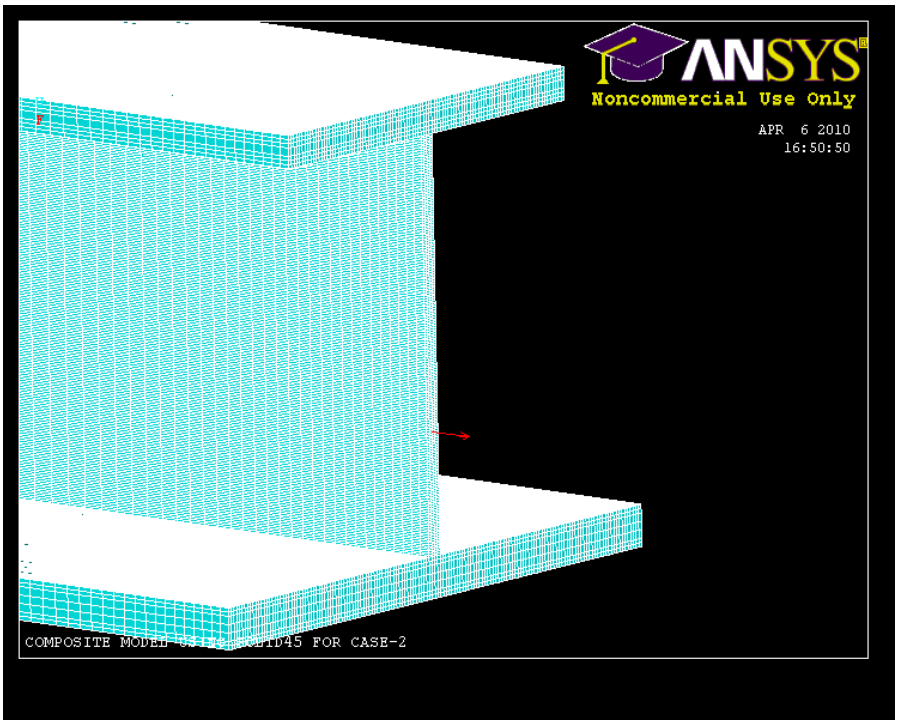

Figure 5.2 $\overline{N_x}$ Applied at the Centroid of I-section.

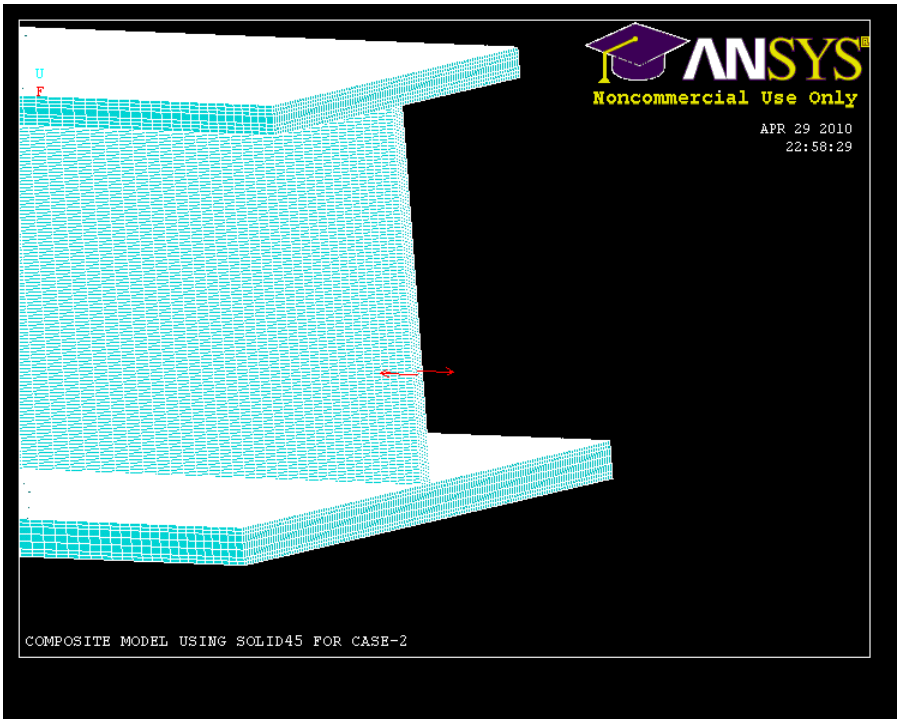

Figure 5.3 Pair of Forces Generating $\overline{M_x}$.

5.2.1 Axial and Bending Stiffnesses of Isotropic Material

The axial stiffness of I-beam was calculated from the finite element model by the following equation.

$$\overline{EA} = \frac{FL}{2\left(U_{x/at\ x=L/2}\right)} \tag{5.2}$$

Where F is the force applied, L is the total length of the beam, and Ux is the axial deflection. For all cases, length of the beam is taken as 10 inches.

To avoid any distortion in axial deflection due to the loading or boundary condition, the deflection results were measured at half way through the length of the beam.

The bending stiffness of I-beam was calculated from the finite element model by determining the curvature of the beam, K_x^c , (See Appendix A) and then dividing the applied moment by it.

$$\overline{M_x} = D_x^c K_x^c$$

$$D_x^c = \frac{\overline{M_x}}{K_x^c}$$

Comparison of the axial and bending stiffnesses for different cases is shown in Table 5.3. The results are excellent agreement with the FEM model. It should be noted that all of I-beams have thicker bottom flange compared to the upper flange. This results in the higher axial stiffness and lower bending stiffness for case 1 compared to the other cases.

Table 5.3 Comparison of Axial and Bending Stiffnesses of Isotropic I-Beam

CASE		UNITS	Theoretical Method	Present method	% Diff	FEM	% Diff
1	$\overline{EA}$	lb	714,000	712,910	-0.15	714,132	0.02
	D_X	lb-in^2	30,457	30,405	-0.17	30,507	0.16
2	$\overline{EA}$	lb	688,500	687,410	-0.16	688,382	-0.02
	D_X	lb-in^2	42,381	42,319	-0.15	42,302	-0.19
3	$\overline{EA}$	lb	680,340	679,240	-0.16	680,170	-0.02
	D_X	lb-in^2	44,737	44,668	-0.15	44,360	-0.84

5.2.2 Equivalent Axial and Bending Stiffnesses of Laminated I-Beam

For a laminated I-beam, Table 5.4 lists the comparison of axial and bending stiffnesses for different I-beams. Same procedure explained above is followed to calculate the axial and bending for the composite beam.

As expected, equivalent axial stiffness increases and the equivalent bending stiffness decreases with increase in width of sub-laminate-2 (bottom flange).

Table 5.4 Comparison of Equivalent Axial and Bending Stiffnesses of Laminated I-Beam

CASE		UNITS	Present method	FEM	% Diff
1	$\overline{EA}$	lb	672,250	664,540	1.16
	D_X	lb-in^2	23,886	23,869	0.07
2	$\overline{EA}$	lb	618,170	612,040	1.00
	D_X	lb-in^2	37,024	36,892	0.36
3	$\overline{EA}$	lb	595,460	589,810	0.96
	D_X	lb-in^2	40,355	39,659	1.75

5.3 Results Comparison of Ply Stresses and Strains of I-Beam

The stresses and strains in plies of sub-laminates of a laminated composite is calculated using method explained in Chapter 3 with the finite element model. Only one case of cross-section is considered for the comparison. The stresses in the plies are calculated in their respective principal coordinate axis i.e. stresses σ_1, σ_2, τ_{12}.

5.3.1 I-Beam Laminate Ply Stresses under Axial Load, $\overline{N_x}$

The stresses and strains developed in plies of each sub-laminates due to an axial loading at the centroid of the cross-section is compared with the analytical solution developed in Chapter 3. Only Case 2 dimensions of I-section is selected to perform the analysis. The stresses in plies of the finite element model are obtained in their respective principal coordinate system. This is done by selecting all the elements of a particular ply and obtaining the stresses using RSYS command. RSYS command in ANSYS displays the results in particular coordinate system; local coordinate system of elements in each ply are chosen for obtaining results for the respective ply. The stresses from analytical expression for each sub laminated are confirmed from the FEM results (Table 5.5 through Table 5.7).

Table 5.5 Comparison of Stresses in Top Flange in Principal Axis due to Axial Load at Centroid

			Sigma 1	%Diff	Sigma 2	%Diff	Tho 12	%Diff
			lb/in^2		lb/in^2		lb/in^2	
Ply #1	45^0	Present Method	1260.20		113.40		-183.00	
		FEM	1344.00	6.24	122.22	7.22	-193.25	5.30
Ply #2	-45^0	Present Method	1260.20		113.40		183.00	
		FEM	1348.10	6.52	123.00	7.80	197.34	7.27
Ply #3	0^0	Present Method	3515.20		-12.90		0.00	
		FEM	3777.00	6.93	-12.16	-6.10	0.02	exact
Ply #4 & Ply#5	90^0	Present Method	-994.80		239.80		0.00	
		FEM	-1065.70	6.65	258.49	7.23	0.07	exact
Ply #6	0^0	Present Method	3515.20		-12.90		0.00	
		FEM	3782.60	7.07	-13.85	6.86	-0.07	exact
Ply #7	-45^0	Present Method	1260.20		113.40		183.00	
		FEM	1357.20	7.15	121.93	7.00	197.22	7.21
Ply #8	45^0	Present Method	1260.20		113.40		-183.00	
		FEM	1351.90	6.78	122.10	7.13	-197.48	7.33

Table 5.6 Comparison of Stresses in Bottom Flange in Principal Axis due to Axial Load at Centroid

			Sigma 1	%Diff	Sigma 2	%Diff	Tho 12	%Diff
			lb/in^2		lb/in^2		lb/in^2	
Ply #1	45^0	Present Method	1263.90		113.80		-182.70	
		FEM	1239.80	-1.94	111.45	-2.11	-178.50	-2.35
Ply #2	-45^0	Present Method	1263.90		113.80		182.70	
		FEM	1238.40	-2.06	111.60	-1.97	178.70	-2.24
Ply #3 & 4	0^0	Present Method	3515.40		-12.40		0.00	
		FEM	3444.60	-2.06	-11.91	-4.11	0.05	exact
Ply #5 & 6	90^0	Present Method	-987.60		239.90		0.00	
		FEM	-967.74	-2.05	235.50	-1.87	0.01	exact
Ply #7 & 8	0^0	Present Method	3515.40		-12.40		0.00	
		FEM	3456.40	-1.71	-12.22	-1.47	0.03	exact
Ply #9	-45^0	Present Method	1263.90		113.80		182.70	
		FEM	1243.80	-1.62	111.83	-1.76	180.08	-1.45
Ply #10	45^0	Present Method	1263.90		113.80		-182.70	
		FEM	1242.10	-1.76	111.98	-1.63	-180.30	-1.33

Table 5.7 Comparison of Stresses in Web Laminate in Principal Axis due to Axial Load at Centroid

			Sigma 1	%Diff	Sigma 2	%Diff	Tho 12	%Diff
			lb/in^2		lb/in^2		lb/in^2	
Ply #1	45^0	Present Method	451.74		40.66		-246.21	
		FEM	463.65	2.57	41.45	1.91	-253.67	2.94
Ply #2	-45^0	Present Method	451.74		40.66		246.21	
		FEM	462.35	2.29	41.85	2.84	253.55	2.90
Ply #3	-45^0	Present Method	451.74		40.66		246.21	
		FEM	464.99	2.85	41.85	2.84	253.42	2.85
Ply #4	-43^0	Present Method	451.74		40.66		-246.21	
		FEM	465.65	2.99	42.06	3.33	-253.29	2.80

The percentage increase in transverse and shear stresses is due to exaggeration; in fact the difference in values is small compared to the axial stress.

5.3.2 I-Beam Laminate Ply Stresses under Bending Moment, $\overline{M_x}$

For laminated I-beam the stresses and strains are calculated using the same method as explained in Section 5.3.1. A moment is generated at the centroid by applying a pair of opposite axial forces at a distance of one ply from the centroid. The axial stresses and strains perfectly match with finite element model results. However, again the transverse and shear stresses and strains are magnified. Table 5.8 through 5.9 shows the comparison of stresses in sub-laminates.

Table 5.8 Comparison of Stresses in Top Flange in Principal Axis due to Bending Moment at Centroid

			Sigma 1	%Diff	Sigma 2	%Diff	Tho 12	%Diff
			lb/in^2		lb/in^2		lb/in^2	
Ply #1	45^0	Present Method	38.36		3.41		-5.33	
		FEM	41.60	7.79	3.84	11.23	-5.24	-1.72
Ply #2	-45^0	Present Method	38.11		3.46		5.42	
		FEM	40.55	6.02	3.66	5.36	5.62	3.56
Ply #3	0^0	Present Method	106.53		-0.33		0.01	
		FEM	111.01	4.04	-0.31	-5.81	-0.01	225.71
Ply #4 & Ply#5	90^0	Present Method	-30.11		7.37		0.00	
		FEM	-31.18	3.43	7.70	4.32	0.00	100.00
Ply #6	0^0	Present Method	110.66		-0.44		0.00	
		FEM	115.42	4.12	-0.46	5.00	0.00	-37.50
Ply #7	-45^0	Present Method	39.89		3.57		5.87	
		FEM	41.35	3.52	3.71	3.83	6.13	4.31
Ply #8	45^0	Present Method	39.79		3.62		-5.96	
		FEM	41.42	3.94	3.73	3.08	-6.23	4.41

Table 5.9 Comparison of Stresses in Bottom Flange in Principal Axis due to Bending Moment at Centroid

			Sigma 1	%Diff	Sigma 2	%Diff	Tho 12	%Diff
			lb/in^2		lb/in^2		lb/in^2	
Ply #1	45^0	Present Method	-19.02		-1.74		3.16	
		FEM	-18.40	-3.35	-1.68	-3.76	3.02	-4.54
Ply #2	-45^0	Present Method	-19.18		-1.70		-3.05	
		FEM	-18.44	-4.01	-1.64	-3.66	-2.92	-4.45
Ply #3 & 4	0^0	Present Method	-55.14		0.34		0.01	
		FEM	-52.83	-4.37	0.31	-9.68	0.01	exact
Ply #5 & 6	90^0	Present Method	15.32		-3.55		0.00	
		FEM	14.61	-4.86	-3.39	-4.63	0.00	exact
Ply #7 & 8	0^0	Present Method	-47.66		0.07		-0.01	
		FEM	-46.92	-1.57	0.11	37.27	0.00	exact
Ply #9	-45^0	Present Method	-17.48		-1.59		-2.32	
		FEM	-16.61	-5.24	-1.51	-5.40	-2.21	-4.84
Ply #10	45^0	Present Method	-17.57		-1.56		2.21	
		FEM	-16.66	-5.43	-1.50	-3.81	1.93	-14.61

5.4 Results Comparison of Ply Stresses in 0^0 ply in Flange Laminates

The stresses in 0^0 ply in sub-laminates of I-beam developed due to axial and bending load is compared for different cases. As expected maximum stress occurs in 0^0 ply in both laminates (sub-laminate 1&2).The 0^0 ply in sub-laminates provide the pure axial stiffness to the I-beams; therefore the stresses are compared to determine the effect of variation in width of flange on the stresses in 0^0 ply of I-beam.

Table 5.10 Comparison of Local Stress in 0^0 Ply due to Axial Load at Centroid

	Top Flange	Bottom Flange
	psi	psi
Case 1	3232.6	3232.6
Case 2	3515.4	3515.2
Case 3	3649.3	3649.4

As expected, the axial stress in 0^0 ply for both top and bottom flange laminates are equal in each case.

Table 5.11 Comparison of Local Stress in 0^0 Ply due to Bending Moment at Centroid

	Top Flange	Bottom Flange
	psi	psi
Case 1	207.88	-37.52
Case 2	110.665	-47.656
Case 3	89.47	-55.77

Here again, the stress in 0^0 ply in the top flange laminate increases and the bottom flange decreases as the centroid of the cross-section moves down.

CHAPTER 6

CONCLUSIVE SUMMARY AND FUTURE WORK

An analytical method was developed for stress analysis of composite I-beam. Approximate closed-form solution was developed to calculate sectional properties such as centroid, equivalent axial and bending stiffness. Finally, the stress and strain in each ply of laminates is calculated using sectional properties. A finite element model is created to obtain the stiffness of each ply. The results of finite element method were compared with analytical solution. Three different cross-section configurations were used to compare and validate the analytical solution.

From this research, following conclusion can be made.

- Analytical expression to calculate centroid shows excellent agreement when validate using isotropic material.
- Equivalent axial and bending stiffnesses obtained from finite element model showed excellent agreement with analytical expression for all three configurations.
- The stress and strain in each ply of I-beam subjected to axial and bending load at the centroid had a difference ranging from negligible to 8% compared to finite element results.
- The 0^0 ply in the top and bottom flange laminates had the maximum stresses for both axial and bending moment loads.
- The axial stress in 0^0 ply, due to axial load at the centroid, was at its maximum for the I-beam with equal width of both flanges compared to uneven width of the flanges.
- The axial stress in 0^0 ply due to bending moment at the centroid was at its maximum for case 1 compared to others 2 configurations.

The new method developed provide excellent alternative for FEM techniques in doing parametric study. The present method can be extended for composite beam with other cross-section such as C-beams. The present method can be extended for the I-beam under torsional load, hygrothermal condition and shear center.

APPENDIX A

CALCULATION OF RADIUS OF CURVATURE FROM FINITE ELEMENT MODEL [17]

Any three points on a line can be selected to determine the curvature of the line from the finite element model under bending by using geometrical calculation. Let Points A, B, and C in Figure A.1 represent three arbitrary points on the line in finite element model with the following coordinates (x_1,y_1), (x_2,y_2), and (x_3,y_3) respectively.

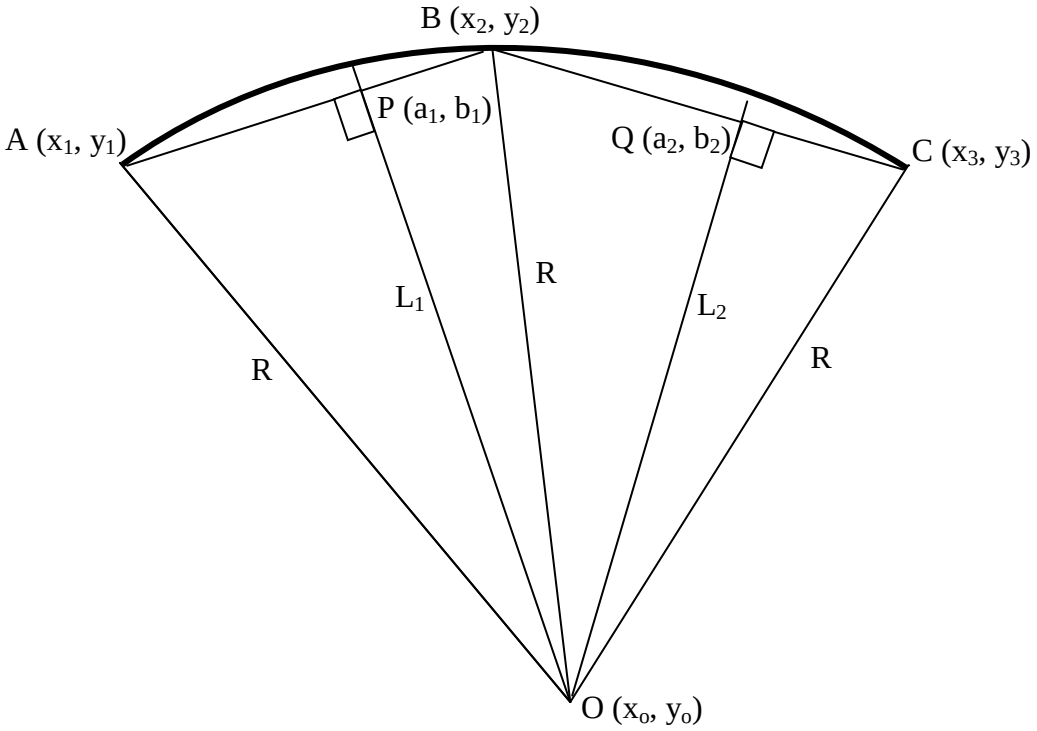

Figure A.1 Three Points Represented on the Curvature.

The center of the curvature is represented by point O with coordinates (x, y). Using the coordinates of points A and B the slope and center point of line AB can be defined as

Slope of Line AB,

$$S_{AB} = \frac{y_2 - y_1}{x_2 - x_1}$$

Center point P,

$$P(a_1, b_1) = \left(\frac{x_1 + x_2}{2}, \frac{y_1 + y_2}{2}\right)$$

The equation of the line L1 which is perpendicular to line AB at point P can be expressed as

$$S_{L1}x - y = S_{L1}a_1 - b_1$$

Where,

$$S_{L1} = -\frac{1}{Slope\ of\ line\ AB} = -\frac{1}{S_{AB}}$$

Similarly, using the same procedure the equation of line L_2 , perpendicular to line BC at point Q, can be expressed as

$$S_{L2}x - y = S_{L2}a_2 - b_2$$

Where,

$$S_{L2} = -\frac{1}{Slope\ of\ line\ BC} = -\frac{1}{S_{BC}}$$

$$N(a_2, b_2) = \left(\frac{x_2 + x_3}{2}, \frac{y_2 + y_3}{2}\right)$$

Line L_1 and L_2 intersect at the center of the curve and the coordinates of point O can be obtained by solving the equation of lines L_1 and L_2. The coordinates of center O can be expressed as

$$x_0 = \frac{S_{L1}a_1 - S_{L2}a_2 - b_1 + b_2}{S_{L1} - S_{L2}}$$

$$y_0 = \frac{S_{L1}S_{L2}(a_1 - a_2) - S_{L1}b_1 + S_{L2}b_2}{S_{L1} - S_{L2}}$$

The distance from the center point O to any of the points A, B, and C is the radius of the curvature of the curve ABC. The radius of curvature can be expressed as,

$$R = \sqrt{(x_0 - x_1)^2 + (y_0 - y_1)^2} = \sqrt{(x_0 - x_2)^2 + (y_0 - y_2)^2} = \sqrt{(x_0 - x_3)^2 + (y_0 - y_3)^2}$$

$$\kappa = \frac{1}{R}$$

APPENDIX B

BATCH MODE ANSYS INPUT DATA FILE FOR FINITE ELEMENT MODEL

```
/TITLE,FINITE ELEMENT COMPOSITE MODEL USING SOLID45
/NOPR
/PMETH,OFF,0
KEYW,PR_SET,1
KEYW,PR_STRUC,1
KEYW,PR_THERM,0
KEYW,PR_FLUID,0
KEYW,PR_ELMAG,0
KEYW,MAGNOD,0
KEYW,MAGEDG,0
KEYW,MAGHFE,0
KEYW,MAGELC,0
KEYW,PR_MULTI,0
KEYW,PR_CFD,0
!
/PREP7
!-----------------------------------------------------
!             MATERIAL PROPERTIES
!-----------------------------------------------------
MPTEMP,,,,,,,,
MPTEMP,1,0
MPDATA,EX,1,,21.75e6
MPDATA,EY,1,,1.595e6
MPDATA,EZ,1,,1.595e6
MPDATA,PRXY,1,,.25
MPDATA,PRYZ,1,,.45
MPDATA,PRXZ,1,,.25
MPDATA,GXY,1,,.8702e6
MPDATA,GYZ,1,,.5366e6
MPDATA,GXZ,1,,.8702e6
!
!-----------------------------------------------------
!             MODEL DIMENSION
!-----------------------------------------------------
L=10                            ! LENGTH OF BEAM
D=20                            ! NO. OF ELEMENT DIVISIONS ON LENGTH OF BEAM
F1=0.5                          ! WIDTH OF SUB-LAMINATE-1
F2=0.75                         ! WIDTH OF SUB-LAMINATE-2
HW=0.5                          ! HEIGTH OF SUB-LAMINATE-3
n1=8                            ! NO. OF LAYERS IN SUB-LAMINATE-1
n2=10                           ! NO. OF LAYERS IN SUB-LAMINATE-2
nw=4                            ! NO. OF LAYERS IN SUB-LAMINATE-3
t=0.005                         ! THICKNESS OF A LAMINATE PLY
!
!-----------------------------------------------------
!             ELEMENT SELECTION
!-----------------------------------------------------
ET,1,PLANE42
ET,2,SOLID45
!
!
!
```

```
!-------------------------------------------------------------------------------------------------------
!               LOCAL CORDINATES SYSTEM FOR FIBER ORIENTATION
!-------------------------------------------------------------------------------------------------------
!
!-----------------------------------------------------
!               FOR SUB-LAMINATE 1(TOP FLANGE)
!-----------------------------------------------------
!
LOCAL,11,,0,0,0,45
LOCAL,12,,0,0,0,-45
LOCAL,13,,0,0,0,0
!
LOCAL,14,,0,0,0,90
!
LOCAL,15,,0,0,0,0
LOCAL,16,,0,0,0,-45
LOCAL,17,,0,0,0,45
!-----------------------------------------------------
!               FOR SUB-LAMINATE 3 (WEB)
!-----------------------------------------------------
!
LOCAL,18,0,0,(F1/2-nw*t/2),0,0,-90,0,1,1,                       ! FOR MODELING AREA
CLOCAL,19,0,0,0,0,45
CSYS,18
CLOCAL,20,0,0,0,0,-45
CSYS,18
CLOCAL,21,0,0,0,0,-45
CSYS,18
CLOCAL,22,0,0,0,0,45
CSYS,0
!-----------------------------------------------------
!               FOR SUB-LAMINATE 2 (BOTTOM FLANGE)
!-----------------------------------------------------
!
LOCAL,23,,0,(F1-F2)/2,-(HW+n2*t)                                ! FOR MODELING AREA
LOCAL,24,,0,0,0,45
LOCAL,25,,0,0,0,-45
!
LOCAL,26,,0,0,0,0
!
LOCAL,27,,0,0,0,90
!
LOCAL,28,,0,0,0,0
!
LOCAL,29,,0,0,0,-45
LOCAL,30,,0,0,0,45
CSYS,0
!-----------------------------------------------------
!               MODELLING SUB-LAMINATE 1
!-----------------------------------------------------
!
K,1,0,0,0,
```

```
K,2,L,0,0,
K,3,L,F1,0,
K,4,0,F1,0,
A,1,2,3,4
!---------------------------------------------------------
!              MESH CONTROL
!---------------------------------------------------------
!
LSEL,S,LINE,,1,3,2
LESIZE,ALL, , ,L*D,-10, , , ,1
LSEL,S,LINE,,2,4,2
LESIZE,ALL,0.005, , , , , , ,1
!---------------------------------------------------------
!              AREA MESH
!---------------------------------------------------------
!
TYPE,   1
MAT,      1
REAL,
ESYS,      0
!
!
CM,_Y,AREA
ASEL, , , ,       1
CM,_Y1,AREA
CHKMSH,'AREA'
CMSEL,S,_Y
!*
MSHKEY,1
AMESH,_Y1
MSHKEY,0
!*
CMDELE,_Y
CMDELE,_Y1
CMDELE,_Y2
!
!---------------------------------------------------------
!              CREATING LAYERS IN SUB-LAMINATE 1
!---------------------------------------------------------
!
TYPE,   2
EXTOPT,ESIZE,1,0,
EXTOPT,ACLEAR,1
EXTOPT,ATTR,0,0,0
MAT,1
REAL,_Z4
ESYS,11
ASEL,S,AREA,,1
VEXT,ALL, , ,0,0,0.005,,,,
ALLSEL
!
TYPE,   2
```

```
EXTOPT,ESIZE,1,0,
EXTOPT,ACLEAR,1
EXTOPT,ATTR,0,0,0
MAT,1
REAL,_Z4
ESYS,12
ASEL,S,LOC,Z,0.005
VEXT,ALL, , ,0,0,0.005,,,,
ALLSEL
!
TYPE,   2
EXTOPT,ESIZE,1,0,
EXTOPT,ACLEAR,1
EXTOPT,ATTR,0,0,0
MAT,1
REAL,_Z4
ESYS,13
ASEL,S,LOC,Z,0.01
VEXT,ALL, , ,0,0,0.005,,,,
ALLSEL
!
TYPE,   2
EXTOPT,ESIZE,1,0,
EXTOPT,ACLEAR,1
EXTOPT,ATTR,0,0,0
MAT,1
REAL,_Z4
ESYS,14
ASEL,S,LOC,Z,0.015
VEXT,ALL, , ,0,0,0.01,,,,
ALLSEL
!
TYPE,   2
EXTOPT,ESIZE,1,0,
EXTOPT,ACLEAR,1
EXTOPT,ATTR,0,0,0
MAT,1
REAL,_Z4
ESYS,15
ASEL,S,LOC,Z,0.025
VEXT,ALL, , ,0,0,0.005,,,,
ALLSEL
!
TYPE,   2
EXTOPT,ESIZE,1,0,
EXTOPT,ACLEAR,1
EXTOPT,ATTR,0,0,0
MAT,1
REAL,_Z4
ESYS,16
ASEL,S,LOC,Z,0.03
VEXT,ALL, , ,0,0,0.005,,,,
```

```
ALLSEL
!
!
TYPE,   2
EXTOPT,ESIZE,1,0,
EXTOPT,ACLEAR,1
EXTOPT,ATTR,0,0,0
MAT,1
REAL,_Z4
ESYS,17
ASEL,S,LOC,Z,0.035
VEXT,ALL, , ,0,0,0.005,,,,
ALLSEL
!
!-----------------------------------------------------------
!              MODELLING SUB-LAMINATE 3
!-----------------------------------------------------------
CSYS,18
K,33,0,0,0,
K,34,L,0,0,
K,35,L,HW,0,
K,36,0,HW,0,
A,33,34,35,36
!
FLST,2,1,5,ORDE,1
FITEM,2,37
VEXT,P51X, , ,0,0,0.005,,,,
!
!-----------------------------------------------------------
!              MESH CONTROL
!-----------------------------------------------------------
LSEL,S,LINE,,61,67,2
LESIZE,ALL, , ,L*D,-10, , , ,1
LSEL,S,LINE,,62,68,2
LESIZE,ALL,0.0025, , , , , , ,1
LSEL,S,LINE,,69,72,1
LESIZE,ALL, , ,1, ,1, , ,1,
!
!
!
!-----------------------------------------------------------
!              CREATING LAYERS IN SUB-LAMINATE 3
!-----------------------------------------------------------
!
TYPE,   2
MAT,      1
REAL,
ESYS,     19
SECNUM,
!*
CM,_Y,VOLU
VSEL, , , ,      8
```

```
CM,_Y1,VOLU
CHKMSH,'VOLU'
CMSEL,S,_Y
!*
MSHAPE,0,3d
MSHKEY,1
VMESH,_Y1
MSHKEY,0
!*
CMDELE,_Y
CMDELE,_Y1
CMDELE,_Y2
!
!
TYPE,   2
EXTOPT,ESIZE,1,0,
EXTOPT,ACLEAR,1
EXTOPT,ATTR,0,0,0
MAT,1
REAL,_Z4
ESYS,20
ASEL,S,LOC,Z,0.005
VEXT,ALL, , ,0,0,0.005,,,,
ALLSEL
!
TYPE,   2
EXTOPT,ESIZE,1,0,
EXTOPT,ACLEAR,1
EXTOPT,ATTR,0,0,0
MAT,1
REAL,_Z4
ESYS,21
ASEL,S, , ,      43
VEXT,ALL, , ,0,0,0.005,,,,
ALLSEL
!
!
TYPE,   2
EXTOPT,ESIZE,1,0,
EXTOPT,ACLEAR,1
EXTOPT,ATTR,0,0,0
MAT,1
REAL,_Z4
ESYS,22
ASEL,S, , ,      48
VEXT,ALL, , ,0,0,0.005,,,,
ALLSEL
!
!-------------------------------------------------------
!              MODELLING SUB-LAMINATE 2
!-------------------------------------------------------
!
```

```
CSYS,23
!
K,53,0,0,0,
K,54,L,0,0,
K,55,L,F2,0,
K,56,0,F2,0,
A,53,54,55,56
!
!-----------------------------------------------------
!               MESH CONTROL
!-----------------------------------------------------
!
LSEL,S,LINE,,97,99,2
LESIZE,ALL, , ,L*D,-10, , , ,1
LSEL,S,LINE,,98,100,2
LESIZE,ALL,0.005, , , , , , ,1
!
!-----------------------------------------------------
!              CREATING LAYERS IN SUB-LAMINATE 3
!-----------------------------------------------------
TYPE,   1
MAT,      1
REAL,
ESYS,     23
SECNUM,
!*
CM,_Y,AREA
ASEL, , , ,     58
CM,_Y1,AREA
CHKMSH,'AREA'
CMSEL,S,_Y
!*
!*
ACLEAR,_Y1
MSHKEY,1
AMESH,_Y1
MSHKEY,0
!*
CMDELE,_Y
CMDELE,_Y1
CMDELE,_Y2
ALLSEL
!
!
TYPE,   2
EXTOPT,ESIZE,1,0,
EXTOPT,ACLEAR,1
EXTOPT,ATTR,0,0,0
MAT,1
REAL,_Z4
ESYS,24
ASEL,S, , ,     58
```

```
VEXT,ALL, , ,0,0,0.005,,,,
ALLSEL
!
!
TYPE,   2
EXTOPT,ESIZE,1,0,
EXTOPT,ACLEAR,1
EXTOPT,ATTR,0,0,0
MAT,1
REAL,_Z4
ESYS,25
ASEL,S, , ,      59
VEXT,ALL, , ,0,0,0.005,,,,
ALLSEL
!
!
TYPE,   2
EXTOPT,ESIZE,1,0,
EXTOPT,ACLEAR,1
EXTOPT,ATTR,0,0,0
MAT,1
REAL,_Z4
ESYS,26
ASEL,S, , ,      64
VEXT,ALL, , ,0,0,0.01,,,,
ALLSEL
!
!
TYPE,   2
EXTOPT,ESIZE,1,0,
EXTOPT,ACLEAR,1
EXTOPT,ATTR,0,0,0
MAT,1
REAL,_Z4
ESYS,27
ASEL,S, , ,      69
VEXT,ALL, , ,0,0,0.01,,,,
ALLSEL
!
!TYPE,   2
EXTOPT,ESIZE,1,0,
EXTOPT,ACLEAR,1
EXTOPT,ATTR,0,0,0
MAT,1
REAL,_Z4
ESYS,28
ASEL,S, , ,      74
VEXT,ALL, , ,0,0,0.01,,,,
ALLSEL
!
!
TYPE,   2
```

```
EXTOPT,ESIZE,1,0,
EXTOPT,ACLEAR,1
EXTOPT,ATTR,0,0,0
MAT,1
REAL,_Z4
ESYS,29
ASEL,S, , ,      79
VEXT,ALL, , ,0,0,0.005,,,,
ALLSEL
!
!
TYPE,   2
EXTOPT,ESIZE,1,0,
EXTOPT,ACLEAR,1
EXTOPT,ATTR,0,0,0
MAT,1
REAL,_Z4
ESYS,30
ASEL,S, , ,      84
VEXT,ALL, , ,0,0,0.005,,,,
ALLSEL
!
!
NUMMRG,ALL                    !MERGE ALL ENTITIES
!
```

APPENDIX C

MATLAB CODE FOR ANALYTICAL SOLUTION

```
%%*****************************************************************************************************
                CALCULATING STRESSES IN LAYERS OF COMPOSITE I-BEAM
%% *****************************************************************************************************
clc
clear all
%- - - - - - - - - - - - - - - - - - - - - - - - - - - - - - - - - - - - - - - - - - - - - - - - - - - - -
%%              MATERIAL PROPERTIES
%- - - - - - - - - - - - - - - - - - - - - - - - - - - - - - - - - - - - - - - - - - - - - - - - - - - - -
E1=21.75e6; E2=1.595e6; G12=0.8702e6; V12=0.25;

%- - - - - - - - - - - - - - - - - - - - - - - - - - - - - - - - - - - - - - - - - - - - - - - - - - - - -
%%              FIBER ORIENTATION
%- - - - - - - - - - - - - - - - - - - - - - - - - - - - - - - - - - - - - - - - - - - - - - - - - - - - -
kt=8;                                           % NO. OF LAYERS IN TOP FLANGE
kb=10;                                          % NO. OF LAYERS IN BOTTOM FLANGE
kw=4;                                           % NO. OF LAYERS IN WEB
t=0.005;                                        % THICKNESS OF LAYER

% FIBER ORIENTATION IN SUB-LAMINATE-1
theta_fl_f1=pi/180*[45;-45;0;90;90;0;-45;45];

% FIBER ORIENTATION IN SUB-LAMINATE-2
theta_fl_f2=pi/180*[45;-45;0;0;90;90;0;0;-45;45];

% FIBER ORIENTATION IN SUB-LAMINATE-3
theta_w=pi/180*[45;-45;-45;45];

%- - - - - - - - - - - - - - - - - - - - - - - - - - - - - - - - - - - - - - - - - - - - - - - - - - - - -
%%               FOR 2D ORTHOTROPIC MATERIAL
%- - - - - - - - - - - - - - - - - - - - - - - - - - - - - - - - - - - - - - - - - - - - - - - - - - - - -
S11= 1/E1; S12=-(V12/E1);
S22= 1/E2;
S66= 1/G12;
S=[S11 S12      0
    S12  S22    0
    0    0      S66];
Q=inv(S);

%- - - - - - - - - - - - - - - - - - - - - - - - - - - - - - - - - - - - - - - - - - - - - - - - - - - - -
%%              USING LAMINATION THEORY
%- - - - - - - - - - - - - - - - - - - - - - - - - - - - - - - - - - - - - - - - - - - - - - - - - - - - -
%%               [A], [B], [D] MATRIXES FOR SUB-LAMINATE-1
%- - - - - - - - - - - - - - - - - - - - - - - - - - - - - - - - - - - - - - - - - - - - - - - - - - - - -

A_fl_f1=0;
D_fl_f1=zeros(3);
B_fl_f1=zeros(3);
hkt=zeros(kt+1,1);
for i=1:kt
   m(i,1)=cos(theta_fl_f1(i,1));
   n(i,1)=sin(theta_fl_f1(i,1));
```

```
   Q_fl_f1_1_1(i,1)=
((m(i,1)^4)*Q(1,1))+((n(i,1)^4)*Q(2,2))+((2*(Q(1,2)+2*(Q(3,3)))*(m(i,1)*n(i,1))^2));
   Q_fl_f1_1_2(i,1)= ((Q(1,1)+Q(2,2)-4*Q(3,3))*((m(i,1)*n(i,1))^2))+((Q(1,2))*(m(i,1)^4+n(i,1)^4));
   Q_fl_f1_1_6(i,1)= ((Q(1,1)-Q(1,2)-2*Q(3,3))*((m(i,1))^3)*(n(i,1)))-((Q(2,2)-Q(1,2)-
2*Q(3,3))*((n(i,1))^3)*(m(i,1)));
   Q_fl_f1_2_2(i,1)= (n(i,1)^4)*Q(1,1)+(m(i,1)^4)*Q(2,2)+2*(Q(1,2)+2*Q(3,3))*(m(i,1)*n(i,1))^2;
   Q_fl_f1_2_6(i,1)= ((Q(1,1)-Q(1,2)-2*Q(3,3))*((n(i,1))^3)*(m(i,1)))-((Q(2,2)-Q(1,2)-
2*Q(3,3))*((m(i,1))^3)*(n(i,1)));
   Q_fl_f1_6_6(i,1)= (Q(1,1)+Q(2,2)-2*Q(1,2)-
2*Q(3,3))*(m(i,1)*n(i,1))^2+(Q(3,3))*(m(i,1)^4+n(i,1)^4);
   Q_f_f1=[Q_fl_f1_1_1(i,1)  Q_fl_f1_1_2(i,1)  Q_fl_f1_1_6(i,1)
   Q_fl_f1_1_2(i,1)  Q_fl_f1_2_2(i,1)  Q_fl_f1_2_6(i,1)
   Q_fl_f1_1_6(i,1)  Q_fl_f1_2_6(i,1)  Q_fl_f1_6_6(i,1)]
   hkt(kt+1,1)=(-kt/2*t);
   hkt(kt+1-i,1)=(-(kt/2-i)*t);
   A_fl_f1=A_fl_f1+Q_f_f1*t;
   B_fl_f1=B_fl_f1+.5*Q_f_f1*(((hkt(kt+1-i,1))^2)-((hkt(kt+2-i,1))^2));
   D_fl_f1=D_fl_f1+1/3*Q_f_f1*(((hkt(kt+1-i,1))^3)-((hkt(kt+2-i,1))^3));
end
A_fl_f1
B_fl_f1
D_fl_f1

%- - - - - - - - - - - - - - - - - - - - - - - - - - - - - - - - - - - - - - - - - - - - - -
%%                [A], [B], [D] MATRIXES FOR SUB-LAMINATE-2
%- - - - - - - - - - - - - - - - - - - - - - - - - - - - - - - - - - - - - - - - - - - - - -

A_fl_f2=0;
D_fl_f2=zeros(3);
B_fl_f2=zeros(3);
hkb=zeros(kb+1,1);
for i=1:kb
   m(i,1)=cos(theta_fl_f2(i,1));
   n(i,1)=sin(theta_fl_f2(i,1));
   Q_fl_f2_1_1(i,1)=
((m(i,1)^4)*Q(1,1))+((n(i,1)^4)*Q(2,2))+((2*(Q(1,2)+2*(Q(3,3)))*(m(i,1)*n(i,1))^2));
   Q_fl_f2_1_2(i,1)= ((Q(1,1)+Q(2,2)-4*Q(3,3))*((m(i,1)*n(i,1))^2))+((Q(1,2))*(m(i,1)^4+n(i,1)^4));
   Q_fl_f2_1_6(i,1)= ((Q(1,1)-Q(1,2)-2*Q(3,3))*((m(i,1))^3)*(n(i,1)))-((Q(2,2)-Q(1,2)-
2*Q(3,3))*((n(i,1))^3)*(m(i,1)));
   Q_fl_f2_2_2(i,1)= (n(i,1)^4)*Q(1,1)+(m(i,1)^4)*Q(2,2)+2*(Q(1,2)+2*Q(3,3))*(m(i,1)*n(i,1))^2;
   Q_fl_f2_2_6(i,1)= ((Q(1,1)-Q(1,2)-2*Q(3,3))*((n(i,1))^3)*(m(i,1)))-((Q(2,2)-Q(1,2)-
2*Q(3,3))*((m(i,1))^3)*(n(i,1)));
   Q_fl_f2_6_6(i,1)= (Q(1,1)+Q(2,2)-2*Q(1,2)-
2*Q(3,3))*(m(i,1)*n(i,1))^2+(Q(3,3))*(m(i,1)^4+n(i,1)^4);
   Q_f_f2=[Q_fl_f2_1_1(i,1)  Q_fl_f2_1_2(i,1)  Q_fl_f2_1_6(i,1)
          Q_fl_f2_1_2(i,1)  Q_fl_f2_2_2(i,1)  Q_fl_f2_2_6(i,1)
          Q_fl_f2_1_6(i,1)  Q_fl_f2_2_6(i,1)  Q_fl_f2_6_6(i,1)];
   hkb(kb+1,1)=(-kb/2*t);
   hkb(kb+1-i,1)=(-(kb/2-i)*t);
   A_fl_f2=A_fl_f2+Q_f_f2*t;
   B_fl_f2=B_fl_f2+.5*Q_f_f2*(((hkb(kb+1-i,1))^2)-((hkb(kb+2-i,1))^2));
   D_fl_f2=D_fl_f2+1/3*Q_f_f2*(((hkb(kb+1-i,1))^3)-((hkb(kb+2-i,1))^3));
```

```
end
A_fl_f2
B_fl_f2
D_fl_f2

%- - - - - - - - - - - - - - - - - - - - - - - - - - - - - - - - - - - - - - - - - - - - - - -
%%              [A], [B], [D] MATRIXES FOR SUB-LAMINATE-3
%- - - - - - - - - - - - - - - - - - - - - - - - - - - - - - - - - - - - - - - - - - - - - - -

A_w=0;
D_w=zeros(3);
B_w=zeros(3);
hkw=zeros(kw+1,1);
for i=1:kw
   m(i,1)=cos(theta_w(i,1));
   n(i,1)=sin(theta_w(i,1)) ;
   Q_w_1_1(i,1)=
((m(i,1)^4)*Q(1,1))+((n(i,1)^4)*Q(2,2))+((2*(Q(1,2)+2*(Q(3,3)))*(m(i,1)*n(i,1))^2));
   Q_w_1_2(i,1)= ((Q(1,1)+Q(2,2)-4*Q(3,3))*((m(i,1)*n(i,1))^2))+((Q(1,2))*(m(i,1)^4+n(i,1)^4));
   Q_w_1_6(i,1)= ((Q(1,1)-Q(1,2)-2*Q(3,3))*((m(i,1))^3)*(n(i,1)))-((Q(2,2)-Q(1,2)-
2*Q(3,3))*((n(i,1))^3)*(m(i,1)));
   Q_w_2_2(i,1)= (n(i,1)^4)*Q(1,1)+(m(i,1)^4)*Q(2,2)+2*(Q(1,2)+2*Q(3,3))*(m(i,1)*n(i,1))^2;
   Q_w_2_6(i,1)= ((Q(1,1)-Q(1,2)-2*Q(3,3))*((n(i,1))^3)*(m(i,1)))-((Q(2,2)-Q(1,2)-
2*Q(3,3))*((m(i,1))^3)*(n(i,1)));
   Q_w_6_6(i,1)= (Q(1,1)+Q(2,2)-2*Q(1,2)-
2*Q(3,3))*(m(i,1)*n(i,1))^2+(Q(3,3))*(m(i,1)^4+n(i,1)^4);
   Q_f_w=[Q_w_1_1(i,1)  Q_w_1_2(i,1)  Q_w_1_6(i,1)
          Q_w_1_2(i,1)  Q_w_2_2(i,1)  Q_w_2_6(i,1)
          Q_w_1_6(i,1)  Q_w_2_6(i,1)  Q_w_6_6(i,1)];
   hkw(kw+1,1)=(-kw/2*t);
   hkw(kw+1-i,1)=(-(kw/2-i)*t);
   A_w=A_w+Q_f_w*t;
   B_w=B_w+.5*Q_f_w*(((hkw(kw+1-i,1))^2)-((hkw(kw+2-i,1))^2));
   D_w=D_w+1/3*Q_f_w*(((hkw(kw+1-i,1))^3)-((hkw(kw+2-i,1))^3));
  end
A_w
B_w
D_w

%- - - - - - - - - - - - - - - - - - - - - - - - - - - - - - - - - - - - - - - - - - - - - - -
%%              CENTROID OF I-SECTION COMPOSITE BEAM
%- - - - - - - - - - - - - - - - - - - - - - - - - - - - - - - - - - - - - - - - - - - - - - -

bf_f1=0.5;                                  % BREADTH OF SUB-LAMINATE-1
bf_f2=0.75;                                 % BREADTH OF SUB-LAMINATE-2
hw=0.5;                                     % HEIGTH OF SUB-LAMINATE-3
Z_1=(kb*t)+hw+(0.5*kt*t);
Z_2=(0.5*kb*t);
Z_3=(kb*t)+(0.5*hw);
Z_c_n=((bf_f1*A_fl_f1(1,1)*Z_1)+(bf_f2*A_fl_f2(1,1)*Z_2)+(hw*A_w(1,1)*Z_3));
Z_c_d=((bf_f1*A_fl_f1(1,1))+(bf_f2*A_fl_f2(1,1))+(hw*A_w(1,1)));
Z_c=Z_c_n/Z_c_d
```

```
%- - - - - - - - - - - - - - - - - - - - - - - - - - - - - - - - - - - - - - - - - - - - - - - - - - - - - - - - - - - - - - - - - -
%%              EQUVALENT AXIAL STIFFNESS
%- - - - - - - - - - - - - - - - - - - - - - - - - - - - - - - - - - - - - - - - - - - - - - - - - - - - - - - - - - - - - - - - - -

EA1=((bf_f1*A11_str_f1)+(bf_f2*A11_str_f2)+(hw*A11_str_w))

%- - - - - - - - - - - - - - - - - - - - - - - - - - - - - - - - - - - - - - - - - - - - - - - - - - - - - - - - - - - - - - - - - -
%%              EQUIVALENT BENDING STIFFNESS
%- - - - - - - - - - - - - - - - - - - - - - - - - - - - - - - - - - - - - - - - - - - - - - - - - - - - - - - - - - - - - - - - - -
Z_1c=Z_1-Z_c            % DISTANCE BETWEEN MID-PLANE OF SUB-LAMINATE-1 &
CENTRIOD
Z_2c=(Z_2-Z_c)          % DISTANCE BETWEEN MID-PLANE OF SUB-LAMINATE-2 &
CENTRIOD
hwc=Z_3-Z_c             % DISTANCE BETWEEN MID-PLANE OF SUB-LAMINATE-3 &
CENTRIOD

mx1=bf_f1*((A11_str_f1*Z_1c^2)+(B11_str_f1*2*Z_1c)+(D11_str_f1));
mx2=bf_f2*((A11_str_f2*Z_2c^2)+(B11_str_f2*2*Z_2c)+(D11_str_f2));
mx3=A11_str_w*((1/12*(hw^3))+(hw*(hwc^2)));

DX1=mx1+mx2+mx3

%- - - - - - - - - - - - - - - - - - - - - - - - - - - - - - - - - - - - - - - - - - - - - - - - - - - - - - - - - - - - - - - - - -
%% CONSTITUTIVE EQUATION OF NARROW BEAM
%- - - - - - - - - - - - - - - - - - - - - - - - - - - - - - - - - - - - - - - - - - - - - - - - - - - - - - - - - - - - - - - - - -
%%              FOR SUB-LAMINATE 1
%- - - - - - - - - - - - - - - - - - - - - - - - - - - - - - - - - - - - - - - - - - - - - - - - - - - - - - - - - - - - - - - - - -

K_f1=zeros(6);
K_f1=[A_fl_f1 B_fl_f1;B_fl_f1 D_fl_f1];
K_f1_tr=inv(K_f1);
a_f1=K_f1_tr(1:3,1:3);
b_f1=K_f1_tr(1:3,4:6);
b_t_f1=K_f1_tr(4:6,1:3);
d_f1=K_f1_tr(4:6,4:6);
a11_f1=a_f1(1:1,1:1);
b11_f1=b_f1(1:1,1:1);
b_t11_f1=b_t_f1(1:1,1:1);
d11_f1=d_f1(1:1,1:1);
K1_f1=[a11_f1     b11_f1
       b_t11_f1   d11_f1];
K1_t_f1=inv(K1_f1);
A11_str_f1=K1_t_f1(1,1);
B11_str_f1=K1_t_f1(1,2);
D11_str_f1=K1_t_f1(2,2);

%- - - - - - - - - - - - - - - - - - - - - - - - - - - - - - - - - - - - - - - - - - - - - - - - - - - - - - - - - - - - - - - - - -
%%               FOR SUB-LAMINATE 2
%- - - - - - - - - - - - - - - - - - - - - - - - - - - - - - - - - - - - - - - - - - - - - - - - - - - - - - - - - - - - - - - - - -
```

```
K_f2=zeros(6);
K_f2=[A_fl_f2 B_fl_f2;B_fl_f2 D_fl_f2];
K_f2_tr=inv(K_f2);
a_f2=K_f2_tr(1:3,1:3);
b_f2=K_f2_tr(1:3,4:6);
b_t_f2=K_f2_tr(4:6,1:3);
d_f2=K_f2_tr(4:6,4:6);
a11_f2=a_f2(1:1,1:1);
b11_f2=b_f2(1:1,1:1);
b_t11_f2=b_t_f2(1:1,1:1);
d11_f2=d_f2(1:1,1:1);
K1_f2=[a11_f2     b11_f2
       b_t11_f2   d11_f2];
K1_t_f2=inv(K1_f2);
A11_str_f2=K1_t_f2(1,1);
B11_str_f2=K1_t_f2(1,2);
D11_str_f2=K1_t_f2(2,2);

%- - - - - - - - - - - - - - - - - - - - - - - - - - - - - - - - - - - - - - - - - - - -
%%                  FOR SUB-LAMINATE-3
%- - - - - - - - - - - - - - - - - - - - - - - - - - - - - - - - - - - - - - - - - - - -

K_w=zeros(6);
K_w=[A_w B_w;B_w D_w];
K_w_tr=inv(K_w);
a_w=K_w_tr(1:3,1:3);
b_w=K_w_tr(1:3,4:6);
b_t_w=K_w_tr(4:6,1:3);
d_w=K_w_tr(4:6,4:6);
a11_w=a_w(1:1,1:1);
b11_w=b_w(1:1,1:1);
b_t11_w=b_t_w(1:1,1:1);
d11_w=d_w(1:1,1:1);
K1_w=[a11_w     b11_w
      b_t11_w   d11_w];
K1_t_w=inv(K1_w);
A11_str_w=K1_t_w(1,1);
B11_str_w=K1_t_w(1,2);
D11_str_w=K1_t_w(2,2);
%- - - - - - - - - - - - - - - - - - - - - - - - - - - - - - - - - - - - - - - - - - - - - - - - - - - - - - - - - - - - - - -
%% STRESSES AND STRAINS IN LAMINATES LAYERS DUE TO MOMENT, M ACTING AT
%                                   THE CENTRIOD
%- - - - - - - - - - - - - - - - - - - - - - - - - -  - - - - - - - - - - - - - - - - - - - - - - - - - - - - - - - - - - - -

M=0.5
%- - - - - - - - - - - - - - - - - - - - - - - - - - - - - - - - - - - - - - - - - - - -
%%                 SECTIONAL PROPERTIES
%- - - - - - - - - - - - - - - - - - - - - - - - - - - - - - - - - - - - - - - - - - - -
EA1 =6.1817e+005              % AXIAL STIFFNESS
DX1 =3.7024e+004              %BENDING STIFFNESS
K_x_c=M/DX1                   % MID-PLANE STRAIN AT CENTRIOD
```

```
Z_1c=Z_1-Z_c            % DISTANCE BTW MID-PLANE OF SUB-LAMINATE-1 & CENTRIOD
Z_2c=(Z_2-Z_c)          % DISTANCE BTW MID-PLANE OF SUB-LAMINATE-2 & CENTRIOD
hwc=Z_3-Z_c             % DISTANCE BTW MID-PLANE OF SUB-LAMINATE-3 & CENTRIOD
%- - - - - - - - - - - - - - - - - - - - - - - - - - - - - - - - - - - - - - - - -
%%              FOR SUB-LAMINATES 1
%- - - - - - - - - - - - - - - - - - - - - - - - - - - - - - - - - - - - - - - - -
% Force and Moments
Nx_1_f1=(B11_str_f1+(Z_1c*A11_str_f1))*K_x_c;
Mx_1_f1=(D11_str_f1+(Z_1c*B11_str_f1))*K_x_c;
Mxy_1_f1=(1/d_f1(3,3))*((b_t_f1(1,3)*Nx_1_f1)+(d_f1(1,3)*Mx_1_f1));
F_0_f1=[Nx_1_f1;Mx_1_f1;Mxy_1_f1];

% %  Mid-plane strains and curvature

Ep_0_f1=zeros(3,3);
Ep_0_f1(:,1)=K_f1_tr(1:3,1:1);
Ep_0_f1(:,2)=K_f1_tr(1:3,4:4);
Ep_0_f1(:,3)=K_f1_tr(1:3,5:5);
Ep_0_f1=Ep_0_f1*F_0_f1;

K_0_f1=zeros(3,3);
K_0_f1(:,1)=K_f1_tr(4:6,1:1);
K_0_f1(:,2)=K_f1_tr(4:6,4:4);
K_0_f1(:,3)=K_f1_tr(4:6,5:5);
K_0_f1=K_0_f1*F_0_f1;

Ep_k_f1=zeros(3,kt+1);
Sigma_k_f1=zeros(3,kt+1);

for i=1:kt
   Z_kt=hkt(kt+2-i,1);
   Ep_k_f1(:,kt+2-i)=Ep_0_f1+(Z_kt*K_0_f1)
   m1=theta_fl_f1(i,1);
   n1=theta_fl_f1(i,1);
   m=cos(m1);
   n=sin(n1);
   Q_fl_f1_1_1= ((m^4)*Q(1,1))+((n^4)*Q(2,2))+((2*(Q(1,2)+2*(Q(3,3)))*(m*n)^2));
   Q_fl_f1_1_2= ((Q(1,1)+Q(2,2)-4*Q(3,3))*((m*n)^2))+((Q(1,2))*(m^4+n^4));
   Q_fl_f1_1_6= ((Q(1,1)-Q(1,2)-2*Q(3,3))*((m)^3)*(n))-((Q(2,2)-Q(1,2)-2*Q(3,3))*((n)^3)*(m));
   Q_fl_f1_2_2= (n^4)*Q(1,1)+(m^4)*Q(2,2)+2*(Q(1,2)+2*Q(3,3))*(m*n)^2;
   Q_fl_f1_2_6= ((Q(1,1)-Q(1,2)-2*Q(3,3))*((n)^3)*(m))-((Q(2,2)-Q(1,2)-2*Q(3,3))*((m)^3)*(n));
   Q_fl_f1_6_6= (Q(1,1)+Q(2,2)-2*Q(1,2)-2*Q(3,3))*(m*n)^2+(Q(3,3))*(m^4+n^4);
   Q_f_f1=[Q_fl_f1_1_1  Q_fl_f1_1_2  Q_fl_f1_1_6
         Q_fl_f1_1_2  Q_fl_f1_2_2  Q_fl_f1_2_6
         Q_fl_f1_1_6  Q_fl_f1_2_6  Q_fl_f1_6_6];
Sigma_k_f1(:,kt+2-i)= Q_f_f1*Ep_k_f1(1:3,kt+2-i:kt+2-i);
end

Z_kt=hkt(1,1);
Ep_k_f1(:,1)=Ep_0_f1+(Z_kt*K_0_f1);
Sigma_k_f1(:,1)= Q_f_f1*Ep_k_f1(1:3,1:1);
```

```
%- - - - - - - - - - - - - - - - - - - - - - - - - - - - - - - - - - - - - - - - - - - - - - - - - - -
%%                FOR SUB-LAMINATES-2
%- - - - - - - - - - - - - - - - - - - - - - - - - - - - - - - - - - - - - - - - - - - - - - - - - - -
% Force and Moments
Nx_1_f2=(B11_str_f2+Z_2c*A11_str_f2)*K_x_c;
Mx_1_f2=(D11_str_f2+Z_2c*B11_str_f2)*K_x_c;
Mxy_1_f2=(1/d_f2(3,3))*((b_t_f2(1,3)*Nx_1_f2)+(d_f2(1,3)*Mx_1_f2));

F_0_f2=[Nx_1_f2;Mx_1_f2;Mxy_1_f2];

% Mid-plane strains and curvature

Ep_0_f2=zeros(3,3);
Ep_0_f2(:,1)=K_f2_tr(1:3,1:1);
Ep_0_f2(:,2)=K_f2_tr(1:3,4:4);
Ep_0_f2(:,3)=K_f2_tr(1:3,5:5);
Ep_0_f2=Ep_0_f2*F_0_f2;
K_0_f2=zeros(3,3);
K_0_f2(:,1)=K_f2_tr(4:6,1:1);
K_0_f2(:,2)=K_f2_tr(4:6,4:4);
K_0_f2(:,3)=K_f2_tr(4:6,5:5);
K_0_f2=K_0_f2*F_0_f2;

Ep_k_f2=zeros(3,kb+1);
Sigma_k_f2=zeros(3,kb+1);

for i=1:kb
   Z_kb=hkb(kb+2-i,1);
   Ep_k_f2(:,kb+2-i)=Ep_0_f2+(Z_kb*K_0_f2);
   m2=theta_fl_f2(i,1);
   n2=theta_fl_f2(i,1);
   m=cos(m2);
   n=sin(n2);
   Q_fl_f2_1_1= ((m^4)*Q(1,1))+((n^4)*Q(2,2))+((2*(Q(1,2)+2*(Q(3,3)))*(m*n)^2));
   Q_fl_f2_1_2= ((Q(1,1)+Q(2,2)-4*Q(3,3))*((m*n)^2))+((Q(1,2))*(m^4+n^4));
   Q_fl_f2_1_6= ((Q(1,1)-Q(1,2)-2*Q(3,3))*((m)^3)*(n))-((Q(2,2)-Q(1,2)-2*Q(3,3))*((n)^3)*(m));
   Q_fl_f2_2_2= (n^4)*Q(1,1)+(m^4)*Q(2,2)+2*(Q(1,2)+2*Q(3,3))*(m*n)^2;
   Q_fl_f2_2_6= ((Q(1,1)-Q(1,2)-2*Q(3,3))*((n)^3)*(m))-((Q(2,2)-Q(1,2)-2*Q(3,3))*((m)^3)*(n));
   Q_fl_f2_6_6= (Q(1,1)+Q(2,2)-2*Q(1,2)-2*Q(3,3))*(m*n)^2+(Q(3,3))*(m^4+n^4);
   Q_f_f2=[Q_fl_f2_1_1  Q_fl_f2_1_2  Q_fl_f2_1_6
         Q_fl_f2_1_2  Q_fl_f2_2_2  Q_fl_f2_2_6
         Q_fl_f2_1_6  Q_fl_f2_2_6  Q_fl_f2_6_6];
   Sigma_k_f2(:,kb+2-i)= Q_f_f2*Ep_k_f2(1:3,kb+2-i:kb+2-i);
end
Z_kt=hkb(1,1);
Ep_k_f2(:,1)=Ep_0_f2+(Z_kt*K_0_f2);
Sigma_k_f2(:,1)= Q_f_f2*Ep_k_f2(1:3,1:1);

%- - - - - - - - - - - - - - - - - - - - - - - - - - - - - - - - - - - - - - - - - - - - - - - - - - -
%%                          FOR WEB-LAMINATE-3
%- - - - - - - - - - - - - - - - - - - - - - - - - - - - - - - - - - - - - - - - - - - - - - - - - - -
```

```
% Force and Moments
Nx_1_w=(B11_str_w+hwc*A11_str_w)*K_x_c;
Mx_1_w=(D11_str_w+hwc*B11_str_w)*K_x_c;
Mxy_1_w=(1/d_w(3,3))*((b_t_w(1,3)*Nx_1_w)+(d_w(1,3)*Mx_1_w));

F_0_w=[Nx_1_w;Mx_1_w;Mxy_1_w];

% Mid-plane strains and curvature

Ep_0_w=zeros(3,3);
Ep_0_w(:,1)=K_w_tr(1:3,1:1);
Ep_0_w(:,2)=K_w_tr(1:3,4:4);
Ep_0_w(:,3)=K_w_tr(1:3,5:5);
Ep_0_w=Ep_0_w*F_0_w;

K_0_w=zeros(3,3);
K_0_w(:,1)=K_w_tr(4:6,1:1);
K_0_w(:,2)=K_w_tr(4:6,4:4);
K_0_w(:,3)=K_w_tr(4:6,5:5);
K_0_w=K_0_w*F_0_w;

Ep_k_w=zeros(3,kw+1);
Sigma_k_w=zeros(3,kw+1);

for i=1:kw
   Z_kw=hkw(i+1,1);
   Ep_k_w(:,kw+2-i)=Ep_0_w+(Z_kw*K_0_w);
   m2=theta_w(i,1);
   n2=theta_w(i,1);
   m=cos(m2);
   n=sin(n2);
   Q_fl_w_1_1= ((m^4)*Q(1,1))+((n^4)*Q(2,2))+((2*(Q(1,2)+2*(Q(3,3)))*(m*n)^2));
   Q_fl_w_1_2= ((Q(1,1)+Q(2,2)-4*Q(3,3))*((m*n)^2))+((Q(1,2))*(m^4+n^4));
   Q_fl_w_1_6= ((Q(1,1)-Q(1,2)-2*Q(3,3))*((m)^3)*(n))-((Q(2,2)-Q(1,2)-2*Q(3,3))*((n)^3)*(m));
   Q_fl_w_2_2= (n^4)*Q(1,1)+(m^4)*Q(2,2)+2*(Q(1,2)+2*Q(3,3))*(m*n)^2;
   Q_fl_w_2_6= ((Q(1,1)-Q(1,2)-2*Q(3,3))*((n)^3)*(m))-((Q(2,2)-Q(1,2)-2*Q(3,3))*((m)^3)*(n));
   Q_fl_w_6_6= (Q(1,1)+Q(2,2)-2*Q(1,2)-2*Q(3,3))*(m*n)^2+(Q(3,3))*(m^4+n^4);
   Q_f_w=[Q_fl_w_1_1  Q_fl_w_1_2  Q_fl_w_1_6
          Q_fl_w_1_2  Q_fl_w_2_2  Q_fl_w_2_6
          Q_fl_w_1_6  Q_fl_w_2_6  Q_fl_w_6_6];
   Sigma_k_w(:,kw+2-i)= Q_f_w*Ep_k_w(1:3,kw+2-i:kw+2-i);
end

Z_kt=hkw(1,1);
Ep_k_w(:,1)=Ep_0_w+(Z_kt*K_0_w);
Sigma_k_w(:,1)= Q_f_w*Ep_k_w(1:3,1:1);

%- - - - - - - - - - - - - - - - - - - - - - - - - - - - - - - - - - - - - - - - - - - - - - - - -  - -
%%                         STRESSES IN PRINCIPAL COORDINATES SYSTEM
%- - - - - - - - - - - - - - - - - - - - - - - - - - - - - - - - - - - - - - - - - - - - - - - - -  - -
Sigma_k_f1_pr=zeros(3,kt);
Sigma_k_f2_pr=zeros(3,kb);
```

```
Sigma_k_w_pr=zeros(3,kw);

%- - - - - - - - - - - - - - - - - - - - - - - - - - - - - - - - - - - - - - - - - - -
%%                  SUB-LAMINATE-1
%- - - - - - - - - - - - - - - - - - - - - - - - - - - - - - - - - - - - - - - - - - -

for i=1:kt
   m2=theta_fl_f1(i,1);
   n2=theta_fl_f1(i,1);
   m=cos(m2);
   n=sin(n2);
   T_Sigma=[m^2          n^2       2*m*n
                n^2           m^2      -2*m*n
                -m*n          m*n       (m^2-n^2)];
   Sigma_k_f1_pr(:,i)=T_Sigma*Sigma_k_f1(:,i);
end

%- - - - - - - - - - - - - - - - - - - - - - - - - - - - - - - - - - - - - - - - - - -
%                   SUB-LAMINATE-2
%- - - - - - - - - - - - - - - - - - - - - - - - - - - - - - - - - - - - - - - - - - -

for i=1:kb
   m2=theta_fl_f2(i,1);
   n2=theta_fl_f2(i,1);
   m=cos(m2);
   n=sin(n2);
   T_Sigma=[m^2          n^2       2*m*n
                n^2           m^2      -2*m*n
                -m*n          m*n       (m^2-n^2)];
   Sigma_k_f2_pr(:,i+1)=T_Sigma*Sigma_k_f2(:,i+1);
end
%- - - - - - - - - - - - - - - - - - - - - - - - - - - - - - - - - - - - - - - - - - -
%                   SUB-LAMINATE-3
%- - - - - - - - - - - - - - - - - - - - - - - - - - - - - - - - - - - - - - - - - - -

for i=1:kw
   m2=theta_w(i,1);
   n2=theta_w(i,1);
   m=cos(m2);
   n=sin(n2);
   T_Sigma=[m^2          n^2       2*m*n
                n^2           m^2      -2*m*n
                -m*n          m*n       (m^2-n^2)];
   Sigma_k_w_pr(:,i+1)=T_Sigma*Sigma_k_w(:,i+1);
end
%- - - - - - - - - - - - - - - - - - - - - - - - - - - - - - - - - - - - - - - - - - - - - - - - - - - - - - - - - - - - - -
%%                          VIEWING RESULTS
%- - - - - - - - - - - - - - - - - - - - - - - - - - - - - - - - - - - - - - - - - - - - - - - - - - - - - - - - - - - - - -

%- - - - - - - - - - - - - - - - - - - - - - - - - - - - - - - - - - - - - - - - - - -
%        STRESSES IN LAYERS SUB-LAMINATE-1 (GLOBAL AND LOCAL COORDINATES)
%- - - - - - - - - - - - - - - - - - - - - - - - - - - - - - - - - - - - - - - - - - -
```

```
Sigma_k_f1
Sigma_k_f1_pr

%- - - - - - - - - - - - - - - - - - - - - - - - - - - - - - - - - - - - - - - - - - - -
%        STRESSES IN LAYERS SUB-LAMINATE-2 (GLOBAL AND LOCAL COORDINATES)
%- - - - - - - - - - - - - - - - - - - - - - - - - - - - - - - - - - - - - - - - - - - -
Sigma_k_f2
Sigma_k_f2_pr

%- - - - - - - - - - - - - - - - - - - - - - - - - - - - - - - - - - - - - - - - - - - -
%        STRESSES IN LAYERS SUB-LAMINATE-3 (GLOBAL AND LOCAL COORDINATES)
%- - - - - - - - - - - - - - - - - - - - - - - - - - - - - - - - - - - - - - - - - - - -
Sigma_k_w
Sigma_k_w_pr


%- - - - - - - - - - - - - - - - - - - - - - - - - - - - - - - - - - - - - - - - - - - - - - - - - - - - - - - - - - - - - - - -
%%                STRESSES AND STRAINS IN LAMINATES LAYERS DUE TO AXIAL LOAD,
PX %                         ACTING AT THE CENTRIOD
%- - - - - - - - - - - - - - - - - - - - - - --- - - - - - - - - - - - - - - - - - - - - - - - - - - - - - - - - - - - - - - -
P=100
Ep_x_c=P/EA1                 % MID-PLANE STRAIN AT CENTRIOD



%- - - - - - - - - - - - - - - - - - - - - - - - - - - - - - - - - - - - - - - - - - - -
%%               FOR SUB-LAMINATES 1
%- - - - - - - - - - - - - - - - - - - - - - - - - - - - - - - - - - - - - - - - - - - -

% Force and Moments
Nx_1_f1=(A11_str_f1)*Ep_x_c
Mx_1_f1=(B11_str_f1)*Ep_x_c
Mxy_1_f1=(1/d_f1(3,3))*((b_t_f1(1,3)*Nx_1_f1)+(d_f1(1,3)*Mx_1_f1))

F_0_f1=[Nx_1_f1;Mx_1_f1;Mxy_1_f1]

% %  Mid-plane strains and curvature
Ep_0_f1=zeros(3,3);
Ep_0_f1(:,1)=K_f1_tr(1:3,1:1);
Ep_0_f1(:,2)=K_f1_tr(1:3,4:4);
Ep_0_f1(:,3)=K_f1_tr(1:3,5:5);
Ep_0_f1=Ep_0_f1*F_0_f1;

K_0_f1=zeros(3,3);
K_0_f1(:,1)=K_f1_tr(4:6,1:1);
K_0_f1(:,2)=K_f1_tr(4:6,4:4);
K_0_f1(:,3)=K_f1_tr(4:6,5:5);
K_0_f1=K_0_f1*F_0_f1;

Ep_k_f1=zeros(3,kt+1);
Sigma_k_f1=zeros(3,kt+1);
```

```
for i=1:kt
   Z_kt=hkt(kt+2-i,1);
   Ep_k_f1(:,kt+2-i)=Ep_0_f1+(Z_kt*K_0_f1)
   m1=theta_fl_f1(i,1);
   n1=theta_fl_f1(i,1);
   m=cos(m1);
   n=sin(n1);
   Q_fl_f1_1_1= ((m^4)*Q(1,1))+((n^4)*Q(2,2))+((2*(Q(1,2)+2*(Q(3,3)))*(m*n)^2));
   Q_fl_f1_1_2= ((Q(1,1)+Q(2,2)-4*Q(3,3))*((m*n)^2))+((Q(1,2))*(m^4+n^4));
   Q_fl_f1_1_6= ((Q(1,1)-Q(1,2)-2*Q(3,3))*((m)^3)*(n))-((Q(2,2)-Q(1,2)-2*Q(3,3))*((n)^3)*(m));
   Q_fl_f1_2_2= (n^4)*Q(1,1)+(m^4)*Q(2,2)+2*(Q(1,2)+2*Q(3,3))*(m*n)^2;
   Q_fl_f1_2_6= ((Q(1,1)-Q(1,2)-2*Q(3,3))*((n)^3)*(m))-((Q(2,2)-Q(1,2)-2*Q(3,3))*((m)^3)*(n));
   Q_fl_f1_6_6= (Q(1,1)+Q(2,2)-2*Q(1,2)-2*Q(3,3))*(m*n)^2+(Q(3,3))*(m^4+n^4);
   Q_f_f1=[Q_fl_f1_1_1  Q_fl_f1_1_2  Q_fl_f1_1_6
           Q_fl_f1_1_2  Q_fl_f1_2_2  Q_fl_f1_2_6
           Q_fl_f1_1_6  Q_fl_f1_2_6  Q_fl_f1_6_6];
Sigma_k_f1(:,kt+2-i)= Q_f_f1*Ep_k_f1(1:3,kt+2-i:kt+2-i);
end

Z_kt=hkt(1,1);
Ep_k_f1(:,1)=Ep_0_f1+(Z_kt*K_0_f1);
Sigma_k_f1(:,1)= Q_f_f1*Ep_k_f1(1:3,1:1);

%- - - - - - - - - - - - - - - - - - - - - - - - - - - - - - - - - - - - - - - - - - - - - - -
%%                FOR SUB-LAMINATES-2
%- - - - - - - - - - - - - - - - - - - - - - - - - - - - - - - - - - - - - - - - - - - - - - -

% Force and Moments
Nx_1_f2=(A11_str_f2)*Ep_x_c;
Mx_1_f2=(B11_str_f2)*Ep_x_c;
Mxy_1_f2=(1/d_f2(3,3))*((b_t_f2(1,3)*Nx_1_f2)+(d_f2(1,3)*Mx_1_f2));

F_0_f2=[Nx_1_f2;Mx_1_f2;Mxy_1_f2];

% Mid-plane strains and curvature
Ep_0_f2=zeros(3,3);
Ep_0_f2(:,1)=K_f2_tr(1:3,1:1);
Ep_0_f2(:,2)=K_f2_tr(1:3,4:4);
Ep_0_f2(:,3)=K_f2_tr(1:3,5:5);
Ep_0_f2=Ep_0_f2*F_0_f2;
K_0_f2=zeros(3,3);
K_0_f2(:,1)=K_f2_tr(4:6,1:1);
K_0_f2(:,2)=K_f2_tr(4:6,4:4);
K_0_f2(:,3)=K_f2_tr(4:6,5:5);
K_0_f2=K_0_f2*F_0_f2;

Ep_k_f2=zeros(3,kb+1);
Sigma_k_f2=zeros(3,kb+1);

for i=1:kb
   Z_kb=hkb(kb+2-i,1);
   Ep_k_f2(:,kb+2-i)=Ep_0_f2+(Z_kb*K_0_f2);
```

```
   m2=theta_fl_f2(i,1);
   n2=theta_fl_f2(i,1);
   m=cos(m2);
   n=sin(n2);
   Q_fl_f2_1_1= ((m^4)*Q(1,1))+((n^4)*Q(2,2))+((2*(Q(1,2)+2*(Q(3,3)))*(m*n)^2));
   Q_fl_f2_1_2= ((Q(1,1)+Q(2,2)-4*Q(3,3))*((m*n)^2))+((Q(1,2))*(m^4+n^4));
   Q_fl_f2_1_6= ((Q(1,1)-Q(1,2)-2*Q(3,3))*((m)^3)*(n))-((Q(2,2)-Q(1,2)-2*Q(3,3))*((n)^3)*(m));
   Q_fl_f2_2_2= (n^4)*Q(1,1)+(m^4)*Q(2,2)+2*(Q(1,2)+2*Q(3,3))*(m*n)^2;
   Q_fl_f2_2_6= ((Q(1,1)-Q(1,2)-2*Q(3,3))*((n)^3)*(m))-((Q(2,2)-Q(1,2)-2*Q(3,3))*((m)^3)*(n));
   Q_fl_f2_6_6= (Q(1,1)+Q(2,2)-2*Q(1,2)-2*Q(3,3))*(m*n)^2+(Q(3,3))*(m^4+n^4);
   Q_f_f2=[Q_fl_f2_1_1  Q_fl_f2_1_2  Q_fl_f2_1_6
         Q_fl_f2_1_2  Q_fl_f2_2_2  Q_fl_f2_2_6
         Q_fl_f2_1_6  Q_fl_f2_2_6  Q_fl_f2_6_6];
   Sigma_k_f2(:,kb+2-i)= Q_f_f2*Ep_k_f2(1:3,kb+2-i:kb+2-i);
end
Z_kt=hkb(1,1);
Ep_k_f2(:,1)=Ep_0_f2+(Z_kt*K_0_f2);
Sigma_k_f2(:,1)= Q_f_f2*Ep_k_f2(1:3,1:1);

%- - - - - - - - - - - - - - - - - - - - - - - - - - - - - - - - - - - - - - - - - - - - - - - -
%%                          FOR WEB-LAMINATE-3
%- - - - - - - - - - - - - - - - - - - - - - - - - - - - - - - - - - - - - - - - - - - - - - - -

% Force and Moments
Nx_1_w=(A11_str_w)*Ep_x_c;
Mx_1_w=(B11_str_w)*Ep_x_c;
Mxy_1_w=(1/d_w(3,3))*((b_t_w(1,3)*Nx_1_w)+(d_w(1,3)*Mx_1_w));

F_0_w=[Nx_1_w;Mx_1_w;Mxy_1_w];
% Mid-plane strains and curvature
Ep_0_w=zeros(3,3);
Ep_0_w(:,1)=K_w_tr(1:3,1:1);
Ep_0_w(:,2)=K_w_tr(1:3,4:4);
Ep_0_w(:,3)=K_w_tr(1:3,5:5);
Ep_0_w=Ep_0_w*F_0_w;

K_0_w=zeros(3,3);
K_0_w(:,1)=K_w_tr(4:6,1:1);
K_0_w(:,2)=K_w_tr(4:6,4:4);
K_0_w(:,3)=K_w_tr(4:6,5:5);
K_0_w=K_0_w*F_0_w;

Ep_k_w=zeros(3,kw+1);
Sigma_k_w=zeros(3,kw+1);

for i=1:kw
   Z_kw=hkw(i+1,1);
   Ep_k_w(:,kw+2-i)=Ep_0_w+(Z_kw*K_0_w);
   m2=theta_w(i,1);
   n2=theta_w(i,1);
   m=cos(m2);
   n=sin(n2);
```

```
   Q_fl_w_1_1= ((m^4)*Q(1,1))+((n^4)*Q(2,2))+((2*(Q(1,2)+2*(Q(3,3)))*(m*n)^2));
   Q_fl_w_1_2= ((Q(1,1)+Q(2,2)-4*Q(3,3))*((m*n)^2))+((Q(1,2))*(m^4+n^4));
   Q_fl_w_1_6= ((Q(1,1)-Q(1,2)-2*Q(3,3))*((m)^3)*(n))-((Q(2,2)-Q(1,2)-2*Q(3,3))*((n)^3)*(m));
   Q_fl_w_2_2= (n^4)*Q(1,1)+(m^4)*Q(2,2)+2*(Q(1,2)+2*Q(3,3))*(m*n)^2;
   Q_fl_w_2_6= ((Q(1,1)-Q(1,2)-2*Q(3,3))*((n)^3)*(m))-((Q(2,2)-Q(1,2)-2*Q(3,3))*((m)^3)*(n));
   Q_fl_w_6_6= (Q(1,1)+Q(2,2)-2*Q(1,2)-2*Q(3,3))*(m*n)^2+(Q(3,3))*(m^4+n^4);
   Q_f_w=[Q_fl_w_1_1  Q_fl_w_1_2  Q_fl_w_1_6
        Q_fl_w_1_2  Q_fl_w_2_2  Q_fl_w_2_6
        Q_fl_w_1_6  Q_fl_w_2_6  Q_fl_w_6_6];
   Sigma_k_w(:,kw+2-i)= Q_f_w*Ep_k_w(1:3,kw+2-i:kw+2-i);
end

Z_kt=hkw(1,1);
Ep_k_w(:,1)=Ep_0_w+(Z_kt*K_0_w);
Sigma_k_w(:,1)= Q_f_w*Ep_k_w(1:3,1:1);

%- - - - - - - - - - - - - - - - - - - - - - - - - - - - - - - - - - - - - - - - - - - - - - - - - - - - - - - - - - - - - - -
%%                          STRESSES IN PRINCIPAL COORDINATES SYSTEM
%- - - - - - - - - - - - - - - - - - - - - - - - - - - - - - - - - - - - - - - - - - - - - - - - - - - - - - - - - - - - - - -
Sigma_k_f1_pr=zeros(3,kt);
Sigma_k_f2_pr=zeros(3,kb);
Sigma_k_w_pr=zeros(3,kw);



%- - - - - - - - - - - - - - - - - - - - - - - - - - - - - - - - - - - - - - - - - - - - - -
%%                  SUB-LAMINATE-1
%- - - - - - - - - - - - - - - - - - - - - - - - - - - - - - - - - - - - - - - - - - - - - -

for i=1:kt
   m2=theta_fl_f1(i,1);
   n2=theta_fl_f1(i,1);
   m=cos(m2);
   n=sin(n2);
   T_Sigma=[m^2          n^2       2*m*n
                 n^2           m^2      -2*m*n
                 -m*n          m*n       (m^2-n^2)];
   Sigma_k_f1_pr(:,i)=T_Sigma*Sigma_k_f1(:,i);
end

%- - - - - - - - - - - - - - - - - - - - - - - - - - - - - - - - - - - - - - - - - - - - - -
%                   SUB-LAMINATE-2
%- - - - - - - - - - - - - - - - - - - - - - - - - - - - - - - - - - - - - - - - - - - - - -

for i=1:kb
   m2=theta_fl_f2(i,1);
   n2=theta_fl_f2(i,1);
   m=cos(m2);
   n=sin(n2);
   T_Sigma=[m^2          n^2       2*m*n
                 n^2           m^2      -2*m*n
                 -m*n          m*n       (m^2-n^2)];
```

```
   Sigma_k_f2_pr(:,i+1)=T_Sigma*Sigma_k_f2(:,i+1);
end
%- - - - - - - - - - - - - - - - - - - - - - - - - - - - - - - - - - - - - - - - - - - - - -
%                    SUB-LAMINATE-3
%- - - - - - - - - - - - - - - - - - - - - - - - - - - - - - - - - - - - - - - - - - - - - -

for i=1:kw
   m2=theta_w(i,1);
   n2=theta_w(i,1);
   m=cos(m2);
   n=sin(n2);
   T_Sigma=[m^2          n^2       2*m*n
                n^2           m^2      -2*m*n
                -m*n          m*n       (m^2-n^2)];
   Sigma_k_w_pr(:,i+1)=T_Sigma*Sigma_k_w(:,i+1);
end
%- - - - - - - - - - - - - - - - - - - - - - - - - - - - - - - - - - - - - - - - - - - - - - - - - - - - - - - - - - - - - - - - - - -
%%                             VIEWING RESULTS
%- - - - - - - - - - - - - - - - - - - - - - - - - - - - - - - - - - - - - - - - - - - - - - - - - - - - - - - - - - - - - - - - - - -

%- - - - - - - - - - - - - - - - - - - - - - - - - - - - - - - - - - - - - - - - - - - - - -
%         STRESSES IN LAYERS SUB-LAMINATE-1 (GLOBAL AND LOCAL COORDINATES)
%- - - - - - - - - - - - - - - - - - - - - - - - - - - - - - - - - - - - - - - - - - - - - -
Sigma_k_f1
Sigma_k_f1_pr

%- - - - - - - - - - - - - - - - - - - - - - - - - - - - - - - - - - - - - - - - - - - - - -
%          STRESSES IN LAYERS SUB-LAMINATE-2 (GLOBAL AND LOCAL COORDINATES)
%- - - - - - - - - - - - - - - - - - - - - - - - - - - - - - - - - - - - - - - - - - - - - -
Sigma_k_f2
Sigma_k_f2_pr

%- - - - - - - - - - - - - - - - - - - - - - - - - - - - - - - - - - - - - - - - - - - - - -
%         STRESSES IN LAYERS SUB-LAMINATE-3 (GLOBAL AND LOCAL COORDINATES)
%- - - - - - - - - - - - - - - - - - - - - - - - - - - - - - - - - - - - - - - - - - - - - -
Sigma_k_w
Sigma_k_w_pr
```

REFERENCES

[1] Barbero, E. J., Fu, S. H., and Raftoyiannis, I. “Ultimate bending strength of composite beams.”, Journal of Materials in Civil Engineering Vol.3 No.4, 1991, pp. 292–306.

[2] Drummond, J. A., and Chan, W. S., “Fabrication, Analysis, and Experimentation of a Practically Constructed Laminated Composite I-Beam under Pure Bending”, Journal of Thermoplatic Comosite Materials, May 1999, pp. 177-187.

[3] Craddock, J. N., and Yen, S. C., “The bending stiffness of laminated composite material I-beams”, Composite Engineering Vol. 3 No.11, 1993, pp. 1025–1038.

[4] Chandra, R., and Chopra, I., “Experimental and theoretical analysis of composites I-beams with elastic couplings”, AIAA Journal Vol. 29 No.12, 1991, pp. 2197–2206.

[5] Barbero, E. J., Lopez-Anido, R., and Davalos, J. F., “On the mechanics of thin-walled laminated composite beams.”, Journal of Composite Materials Vol.27 No.8, 1993, pp. 806–829.

[6] Song, O., Librescu, L., and Jeong, N. H., “Static response of thin-walled composite I-beams loaded at their free-end cross section: analytical solution”, Composite Structures Vol.52, 2001, pp. 55–65.

[7] Jung, S. N., and Lee, J. Y., “Closed-form analysis of thin-walled composite I-beams considering non-classical effects.”, Composite Structures Vol.60, 2003, pp. 9–17.

[8] Chan, W. S., and Chou, C. J., “Effects of Delamination and Ply Fiber Waviness on Effective Axial and Bending Stiffnesses in Composite Laminates”, Composite Structures, Vol. 30, pp. 299-306.

[9] Chan, W. S. and Demirhan, K. C., “A Simple Closed Form Solution of Bending Stiffness of Laminated Composite Tubes”, Journal of Reinforced Plastics and Composites, Vol.19 No. 3, 2001.

[10] Rojas, C. A., Syed, K. A., and Chan, W. S., “Structural Response of Composite Truss Beams”, The 22nd Annual Technical Conference of American Society of Composites, Sept. 2007.

[11] Syed, K.A. and Chan, W.S., “Analysis of Hat-Sectioned Reinforced Composite Beams”, Proceedings of American Society of Composites, Sept. 2006.

[12] Rios, G., “A Unified Analysis of Stiffener Reinforced Composite Beams with Arbitrary Cross-Section”, The University of Texas at Arlington, 2009.

[13] Gan, L. H., Ye, L., and Mai, Y. W., “Simulations of mechanical performance of pultruded I-beams with various flange-web conjunctions”, Composites Part B Vol.30, 1999, pp. 423–429.

[14] Daniel, I. M., and Ishai, O, Engineering Mechanics of Composite Materials, 2nd edition, Oxford University Press, New York, 2006.

[15] Release 11.0 Documentation for ANSYS.

[16] Ugural, A. C., and Fenster, S. K., Advanced Strength and Applied Elasticity, 4th edition, Prentice Hall,PTR

[17] Wang, J. S., and Chan, W. S., “Effects of Deflects on the Buckling Load of Rodpack Laminates”, Journal of American Helicopter Society, July 2000.

BIOGRAPHICAL INFORMATION

Jitesh Cherukkadu Parambil received his Bachelor of Engineering in Aeronautical Engineering from Anna University, Chennai, India. He joined UT Arlington in Fall 2007 and started working under Dr. Kent L. Lawrence and Dr. Wen S. Chan in Fall 2008. His research interests include composite material analysis and design, finite element analysis, structural analysis and design, and computer aided engineering. He received his Master of Science degree in Aerospace Engineering from the University of Texas at Arlington in May 2010.